

The metabolites of light: untargeted metabolomic approaches bring new clues to understand light-driven acclimation of intertidal mudflat biofilm.

Caroline Doose (✉ caroline.doose@mnhn.fr)

Muséum National d'Histoire Naturelle <https://orcid.org/0000-0003-3017-2228>

Cédric Hubas

Research Article

Keywords: microphytobenthos, mudflat biofilm, light acclimation, metabolomics, alkanes, fatty acids

Posted Date: July 27th, 2023

DOI: <https://doi.org/10.21203/rs.3.rs-2096966/v2>

License: © ⓘ This work is licensed under a Creative Commons Attribution 4.0 International License.

[Read Full License](#)

The metabolites of light: untargeted metabolomic approaches bring new clues to understand light-driven acclimation of intertidal mudflat biofilm.

Caroline Doose¹, Cédric Hubas¹

¹ *Muséum National d'Histoire Naturelle, UMR BOREA, MNHN-CNRS-UCN-UPMC-IRD-UA, Station Marine de Concarneau, Concarneau, France*

Caroline Doose : caroline.doose@mnhn.fr - orcid : 0000-0003-3017-2228

Cédric Hubas : cedric.hubas@mnhn.fr - orcid : 0000-0002-9110-9292

Abstract

The microphytobenthos (MPB), a microbial community of primary producers, play a key role in coastal ecosystem functioning, particularly in intertidal mudflats. These mudflats experience challenging variations of irradiance, forcing the micro-organisms to develop photoprotective mechanisms to survive and thrive in this dynamic environment. Two major adaptations to light are well described in literature: the excess of light energy dissipation through non-photochemical quenching (NPQ), and the vertical migration in the sediment. These mechanisms trigger a lot of scientific interest, but the biological processes and metabolic mechanisms involved in light-driven vertical migration remain largely unknown. To our knowledge, this study investigates for the first time metabolomic responses of a migrational mudflat biofilm exposed for 30 min to a light gradient of photosynthetically active radiation (PAR) from 50 to 1000 $\mu\text{mol photons m}^{-2} \text{s}^{-1}$. The untargeted metabolomic analysis allowed to identify metabolites involved in two types of responses to light irradiance levels. On the one hand, the production of SFAs and MUFAs, primarily derived from bacteria, indicates a healthy photosynthetic state of MPB under low light (LL) and medium light (ML) conditions. Conversely, when exposed to high light (HL), the MPB experienced light-induced stress, triggering the production of alka(e)nes and fatty alcohols. The physiological and ecological roles of these compounds are poorly described in literature. This study sheds new light on the topic, as it suggests that these compounds may play a crucial and previously unexplored role in light-induced stress acclimation of migrational MPB biofilms. Since alka(e)nes are produced from FAs decarboxylation, these results thus emphasize for the first time the importance of FAs pathways in microphytobenthic biofilms acclimation to light.

Keywords: microphytobenthos, mudflat biofilm, light acclimations, metabolomics, alkanes, fatty acids

Introduction

The microphytobenthos (MPB) inhabiting marine sediments is a microbial community of primary producers playing a key role in shallow coastal environments and estuarine ecosystem functioning (Beninger and Paterson, 2018; Werner et al., 2006). They are notably important as food source for invertebrates, fish and wading birds since they are at the base of the food web and highly contribute to the total primary production (PP) (Macintyre et al., 1996; Underwood and Kromkamp, 1999) . The diatoms, brown

microalgae usually dominating the MPB, can phase their behavior and metabolisms to the strong intertidal environmental variability allowing them to grow and thrive (Perkins et al., 2010; Saburova and Polikarpov, 2003).

Two major adaptations to light are well described in literature. The first consists of dissipating the excess of light energy through physiological non-photochemical quenching (NPQ) of chlorophyll fluorescence such as the xanthophyll cycle (Goss and Lepetit, 2015). In diatoms, this NPQ mechanism mainly involves the de-epoxydation of the diadinoxanthin (Dd) to diatoxanthin (Dt), avoiding oxidative stress generation and damage to the photosystem II (PSII) (Goss and Jakob, 2010). As a second acclimation, the diatom's vertical migration was also shown to be a major photoprotective response to high light irradiances (Laviale et al., 2015). The latter induced downward movement responses, but upward migrations are also observed in laboratory during daytime under moderate irradiance ($120 \mu\text{mol photons m}^{-2} \text{s}^{-1}$) of white light (Barnett et al., 2020). In fact, the photonic irradiation, the wavelength and the spectral quality of the light on which its biological absorption depends, generate luminous stresses that trigger the upward and downward migration of the diatoms to reach the vertical positioning at their optimal light levels (Cartaxana et al., 2011; Jesus et al., 2006; Prins et al., 2020). Other MPB organisms such as euglenoid or cyanobacteria, were also observed to migrate vertically in the sediment (Consalvey et al., 2004; Haro et al., 2019; Hörnlein et al., 2020) and they seem to migrate together, suggesting the existence of triggering mechanisms and/or signalization processes between them.

The MPB, along with the heterotrophic microorganisms of marine biofilms, is embedded in an extracellular polymeric substances (EPS) matrix that is produced by the microorganisms themselves. These polymers not only hold cells and sediment particles together, but they also harbor small metabolites that allow for a diversity of interactions (communication, metabolic cooperation, or competition) between the microorganisms living within the matrix (Elias and Banin, 2012; Flemming and Wingender, 2010; Sutherland, 2017). There is a lack of small matrix compounds characterization in literature (Gaubert-Boussarie et al., 2020), and they certainly play a key role in the synchronization of the MPB organisms' migration. They could be metabolites excreted in response to light or released in the matrix by dead lysed cells. Small compounds and ions absorbed in the matrix can also originate from the surrounding biofilm environment (Hubas et al., 2018; Wotton, 2004) and might influence the MPB migration as well.

The growing use of metabolomic approaches in marine sciences brings new knowledge on the environmental pressures' effect on health and behavior of organisms (Bundy et al., 2009; Dove et al., 2012). These techniques allow notably to identify chemical compounds involved in communication between micro-organisms (Gaillard and Potin, 2014). Thus, the application of metabolomic tools to the marine biofilm can lead to great progress in the understanding of the global MPB light-driven responses. The NPQ mechanisms trigger a lot of scientific interest with numerous studies in literature, but the biological processes and metabolic mechanisms involved in light-driven vertical migration remain largely unknown

(Coelho et al., 2011; Consalvey et al., 2004). The untargeted metabolomic approach could open up new research lines to better understand their mechanisms and possible implications in other cellular metabolic pathways. In this work we exposed a migrational mudflat biofilm for 30 min to a light gradient of photosynthetically active radiation (PAR) from 50 to 1000 $\mu\text{mol photons m}^{-2} \text{s}^{-1}$. To explore the global metabolic responses to the irradiances and identify compounds playing significant roles in the MPB light acclimation, we applied an untargeted metabolomic analysis method previously adapted for MPB in our laboratory (Gaubert-Boussarie et al., 2020).

Methods

Biofilm sampling and acclimatation

Mudflat's MPB biofilm present at the first 2 cm of sediment was sampled at low tide in an empty breeding pond of the Marine Station of Concarneau (France; 47°52.5804'N; 3°55.026'W) in April 2021. This pond is connected to the Concarneau bay so that it fills at high tide and does not completely drain at low tide, letting the muddy sediment surface immersed under 4–5 cm of seawater. The microphytobenthos was largely dominated by communities of epipellic diatoms, especially two large species: *Pleurosigma formosum* and *Gyrosigma balticum* (Gaubert-Boussarie et al., 2020). The biofilm was collected in plastic boxes and left 24h in half obscurity ($\text{PAR} < 6 \mu\text{mol photons m}^{-2} \text{s}^{-1}$) to let it settle.

Light exposure experiment

After 24h of sedimentation, the top 5 mm of the sediment containing the MPB was sampled and re-suspended in 250 ml of filtered seawater. A volume of 6 mL of resuspended biofilm was added in 5 cm diameter Petri dishes and left 24h in half obscurity ($\text{PAR} < 6 \mu\text{mol photons m}^{-2} \text{s}^{-1}$) to let it settle. A number of 5 Petri dishes ($n=5$) were then placed under dark (D), 50, 100 (LL), 250 (ML), 500, 750 and 1000 (HL) $\mu\text{mol photons m}^{-2} \text{s}^{-1}$ where light was generated by Led Lights (SL 3500, white warm, Photon Systems Instruments). After 30 min of exposure, liquid nitrogen was poured in the Petri dishes to immediately freeze the sediment without disturbance. The samples were freeze-dried and stored at -80°C .

Light curve measurements and F_0 measurements

An additional Petri dish per treatment was dedicated to the light response curve measurements before (t_0) and after ($t_{30\text{min}}$) the light exposure. After the light exposure, the biofilm was let in obscurity for 5 minutes before the beginning of the measurements. The latter were realized with a FluorPen FP 110 (PSI) device which measured the effective quantum yields of photosynthesis under increasing light intensities (10; 20; 50; 100; 300; 500 and 1000 $\mu\text{mol photons m}^{-2} \text{s}^{-1}$) PAR with 60s phase duration based on pulse modulated fluorometry (PAM). The relative electron transport rates (rETR) were calculated and rETR vs. irradiance light curves were plotted to determine the photosynthetic parameters of the MPB using the R software following Prins et al. (2020) (Prins et al., 2020) by using the equations of Eilers & Peeters (1988) modified by Silsbe and Kromkamp (2012) (Silsbe and Kromkamp, 2012).

Before this experiments, the biomass variation of MPB at the sediments surface was measured through the minimum of chlorophyll fluorescence (F_0) with the FluorPen FP 110 (PSI) (Du et al., 2010; Jesus et al., 2006). The data are available in the supplementary material (S1) and showed that the MPB vertical migration followed a diurnal cycle.

Pigment analysis

Freeze-dried sediment (30 mg) was weighed in tubes and 2 mL of methanol was added for 15 min, at -25°C in the dark to extract lipophilic pigments. The samples were filtered through 0.2 μm PTFE syringe filters and stored at -20°C in the dark before being analyzed by an Agilent 1260 Infinity HPLC equipped with DAD and FLD detectors. Samples were injected (100 μl) by an automatic sample injector and pigments were separated on a C18 column for reverse phase chromatography (Supelcosil, 25 cm long, 4.6 mm inner diameter) following the (Brotas and Plante-Cuny, 2003) method with a 0.5 ml/min flow rate of solvent A (0.5 M ammonium acetate in methanol and water, 85:15, v:v), B (acetonitrile and water, 90:10, v:v), and C (100% ethyl acetate). After the chromatographic separation, pigments were detected by a UV-VIS photodiode array detector (DAD 1260 VL, 250–900 nm). The absorption spectra and relative retention times were used to determine the peaks using the Agilent OpenLab software. Pigment concentrations were calculated with the corresponding calibration curves of $\beta\beta$ -carotene, canthaxanthin, chlorophyll *a*, chlorophyll *b*, chlorophyll *c2*, diatoxanthin (DT), diadinoxanthin (DD), fucoxanthin and pheophytin *a* standards. The relative abundance of each pigment (%) was obtained from their concentrations in the samples. The de-epoxidation state (DES) was calculated as $\text{DT}/(\text{DD}+\text{DT})\times 100$.

Untargeted metabolomic analysis

The untargeted metabolomic analysis was performed according to the Gaubert-Boussarie method [20]. A 50 mg freeze-dried biofilm sample was resuspended in a 6 ml mixture of methanol (MeOH) and chloroform (CHCl_3) (1:1) in Pyrex tubes using 30 min of sonication. After centrifugation (1,800 g, 10 min), the supernatant corresponding to the organic phase was collected in new clean Pyrex tubes. This extraction step was repeated 3 times and organic phases were pooled. The extracts were placed to dry under N_2 at room temperature and resuspended in 1 mL of MeOH to be fractionated by Solid Phase Extraction (Strata C18-E, 500 mg/6 mL, Phenomenex). The samples were collected in 3 successive elutions: 6 mL of H_2O containing polar compounds, 6 mL of MeOH containing mid-polar compounds and 6 mL of CHCl_3 containing apolar compounds. The polar fraction was not analyzed and discarded to avoid the damages to GC-MS syringe and column caused by high concentration in salts. A volume of 10 μL of adonitol ($0.5 \text{ mg}\cdot\text{mL}^{-1}$ in milliQ H_2O) was added to the MeOH fractions, 20 μL of tricosanoic acid ($0.5 \text{ mg}\cdot\text{mL}^{-1}$ in chloroform) was added to the CHCl_3 fractions and the samples were dried under N_2 before derivatization.

Derivatization

In MeOH fractions, 80 μL of methoxyamine hydrochloride dissolved in pyridine (20 $\text{mg}\cdot\text{mL}^{-1}$) were added to the extracts which were then ultrasonicated for 10 min before incubation for 90 min at 37°C in a thermal rotating incubator (120 rpm). After an evaporation under N_2 to remove the pyridine, 100 μL of BSTFA + 1% TMCS were added. After 10 min of ultrasonication and a short vortex agitation, the samples were re-incubated for 30 min at 37°C in the thermal rotating incubator. To remove the BSTFA/TMCS, the samples were evaporated under N_2 , then resuspended in MeOH to be analyzed by GC-MS in the next 30h.

To derivatize the dried CHCl_3 fractions, 1 mL of BF_3 -MeOH was added to the extracts, which were then placed at 90°C for 10 min. After cooling down at room temperature, 1 mL of milliQ H_2O and 1 mL of CHCl_3 were added. The samples were vortexed and centrifuged (1,800 g, 5 min). The lower phase was collected to be analyzed by GC-MS.

For each fraction, a volume of 25 μL of each sample was pooled before derivatization to create a quality control (QC). Blanks and QC were derivatized following the same protocol as the samples.

GC-MS analysis

The fractions were injected (1 μL) at 250°C and separated with a constant helium flow rate (1 $\text{mL}\cdot\text{min}^{-1}$) on an HP-5ms Ultra Inert column (30 m, 0.25 mm, and 0.25 μm , Agilent Technologies) in a gas chromatograph (7890B GC System- G1513A autosampler, Agilent Technologies) coupled to a mass selective detector (5977B MSD, Agilent Technologies). The mass spectra were obtained under electron ionization mode (70 eV, between 35 and 600 m/z , scan rate of 1.3 $\text{scan}\cdot\text{s}^{-1}$). The run method for the CHCl_3 fractions was established as following: start at 100°C for 1 min, increased by 15°C min^{-1} up to 215°C, by 5°C min^{-1} from 215 to 285°C and by 15°C min^{-1} from 285 to 325°C ended by 3 min post-run at 100°C. For the MeOH fractions, the run method was as follow: start at 80°C for 1 min, increased by 10°C min^{-1} up to 325°C, holding 1 min at the final temperature ended by 3 min post-run at 80°C.

Data treatment

GC-MS

The Agilent data files obtained from GC-MS were converted into mzXML using MSconvert software (Chambers et al., 2012) to be processed on R by the eRah package version 1.1.0 (Domingo-Almenara et al., 2016). The latter realize peak deconvolution (min.peak.width = 2.8 (1.5 for MeOH fractions), min.peak.height = 2,500 (1,500 for MeOH fractions), noise. threshold = 500, avoid.processing.mz = c(73,149,207)), peak alignment (min.spectra.cor = 0.90, max.time.dist = 2 (8 for MeOH fractions), mz.range = 40:600) and missing compounds recovery (recMissComp function, minimum number of samples was set at 3 for CHCl_3 and 5 for MeOH fractions). The compounds dataset obtained was first filtered by a signal/noise ratio of peaks present in blanks superior to 10. Peaks of QC having a coefficient of variation superior to 35% were removed from the data. The compound's annotation was then realized by comparison with the NIST's

mass spectra database and Kovats' index calculation (Van Den Dool and Dec. Kratz, 1963). The relative abundance of each metabolites (%) was obtained from their peaks area in the samples.

Statistical analysis

The object generated by a Multiple Factor Analysis MFA performed on data of pigments, CHCl₃ and MeOH fractions was used to run a Between Class analysis on R under the package ade4 following the original script available on Github (<https://github.com/Hubas-prog/BC-MFA>). The result is named BC-MFA. The normality of the data and the residuals distribution was tested using the Shapiro–Wilk test. When residuals followed a normal distribution, a one-way ANOVA was performed to detect significant light effects on pigments, CHCl₃ and MeOH fractions variations. When normality was not verified, the non-parametric Van der Waerden test was performed with the R package agricolae. The metabolites diversity indexes for the 2 fractions was determined with the chemodiv package.

Results and discussion

Characterization of the MPB's photo-acclimation to the light gradient

The light response curves (LCs) were monitored in the biofilm at t₀ and after 30min of light exposure to the different irradiance levels (Fig.1). All the biofilm's samples were acclimated in the same conditions at t₀. They can be thus considered as the biofilm's initial state and they were statistically treated as replicates (n=7). The photosynthetic activity can be estimated by 4 parameters calculated from the LCs: the maximum relative electron transport rate (rETR_{max}), minimum saturating irradiance (E_k), light utilization coefficient (α) and optimal light parameter (E_{opt}). These parameters were often measured in studies on mudflat biofilms (Chevalier et al., 2010; Herlory et al., 2007; Serôdio et al., 2008). However, the differences of sampling procedures with associated perturbations (resuspension, filtration, centrifugation, light acclimation, etc) make the comparison with the literature difficult (Maggi et al., 2013). In this study, we tried to minimize the biofilm's structural perturbations by avoiding filtering and centrifugation. The measured values at t₀ were in the same range as in field studies (Jordan et al., 2010, 2008) and studies realized in resembling sampling and laboratory conditions (Du et al., 2018; Prins et al., 2020). The E_{opt} observed at t₀ in the MPB was 503± 53 μmol. photons. m⁻².s⁻¹ PAR. This value indicates the threshold of relative electron transport rate (rETR) saturating irradiance at which further increase in light induces photoprotection.

After 30 min of light exposure (t_{30min}), the rETR_{max30min}, E_{k30min} and α_{30min} values observed for the D, 50 and 100 irradiance conditions were not different from the standard deviation range of the t₀ values. The 30 min exposure of light irradiances lower than 250 μmol. photons. m⁻².s⁻¹ had thus no major effect on MPB photophysiology. From 500 to 1000 μmol. photons. m⁻².s⁻¹, lower E_{opt30min} values than those in the t₀ conditions indicated the induction of photoprotection mechanisms. The principal photoprotective mechanism of MPB, alongside with the migration, consists of the thermal dissipation of energy through the

xanthophyll cycle called non-photochemical quenching (NPQ). The value of α are used as a proxy to monitor short-term NPQ level changes (Prins et al., 2020), since the both have been shown to be inversely proportional (Cruz and Serôdio, 2008; Serôdio et al., 2006). From 250 to 1000 $\mu\text{mol photons m}^{-2}\cdot\text{s}^{-1}$, the $\alpha_{30\text{min}}$ values tended to decrease following the light gradient. The decreasing trend of α value indicated that NPQ probably followed the irradiance increase as expected. In diatoms (microalgae dominating the MPB), NPQ mechanism involves the de-epoxydation of the diadinoxanthin (Dd) to the diatoxanthin (Dt) (Goss and Jakob, 2010), where the Dt biosynthesis can be linearly correlated with diatom NPQ (Lavaud, 2007; Lavaud et al., 2004, 2002). The de-epoxidation state index (DES) increased significantly following the light irradiance level (Fig.1, Van der Waerden test, $p < 0.05$) showing an intensification of diatoms' NPQ and along this gradient confirming the trend of α values.

The DES values were significantly higher in the 500, 750 and 1000 than under 50, 100 and 250 $\mu\text{mol photons m}^{-2}\cdot\text{s}^{-1}$ irradiance levels. The decrease of $E_{\text{opt}30\text{min}}$, $r\text{ETR}_{\text{max}30\text{min}}$ and $E_{k30\text{min}}$ values together with the increase of DES suggested a light-induced stress threshold between 250 and 500 $\mu\text{mol photons m}^{-2}\cdot\text{s}^{-1}$. This light-induced stress threshold is consistent with the E_{opt} values of the MPB at t_0 corresponding to the light level for which the photoprotection is induced. Moreover, all the LCs slopes (at t_0 and $t_{30\text{min}}$) appeared to decrease after $r\text{ETR}$ reached the E_{opt} values. This indicates that photoinhibition occurred despite the photoprotection induction. In literature related to MPB, photoinhibition is rarely observed (Blanchard et al., 2004; Mouget et al., 2008; Waring et al., 2007). The studied MPB communities are described to be adapted to a wide range of irradiances through physiological regulation and migration (Cartaxana et al., 2011; Serôdio et al., 2012). But, the photoinhibition was also suggested to be underestimated by *Chl a* fluorescence measurements (Serôdio et al., 2012). Previous studies showed photoinhibition up to 20% under laboratory conditions with irradiances between 500 and 1200 $\mu\text{mol photons m}^{-2}\cdot\text{s}^{-1}$ (Blanchard et al., 2004; Du et al., 2018; Serôdio et al., 2012), and up to 18% observed *in situ* (Serôdio et al., 2008). The photoinhibitory responses observed in the present study could be explained by the low-light conditions provided by the breeding pond leading to a MPB acclimated to low irradiances.

The heterogeneous taxonomic composition of the MPB probably leads to a species-dependent diversity of photoacclimation status (Serôdio et al., 2006). But the measured LCs and their calculated parameters reflect a global response of the MPB to the light irradiances while the DES values reflect the diatom community's response. The light irradiances were gathered in 3 groups (low light, LL; medium light, ML; high light, HL) corresponding to the different levels of photosynthetic activity responses of the MPB (table 1). To simplify the reading of the text, these groups' denominations will be used further in the discussion to refer to light conditions.

Table.1 Groups of light irradiances levels depending on their effect on MPB			
	Low light	Medium Light	High light
Abbreviation	LL	ML	HL
Irradiance ($\mu\text{mol m}^{-2}\cdot\text{s}^{-1}$ PAR)	50 and 100	250	500, 750 and 1000

NPQ	NPQ<PQ*	NPQ>PQ	NPQ>PQ
Photoinhibition	Not induced	Not induced	Induced

*based on EK values which are related to quenching, where photochemical quenching dominates below Ek, while non-photochemical quenching dominates the fluorescence quenching above Ek (Henley, 1993)

Metabolic responses to light irradiance show lipids central role in biofilm light acclimation

To better understand metabolic changes under light irradiance levels, a non-targeted metabolomic analysis was performed on the MPB samples. This method allows the extraction and measurement of a wide variety of polar and semi-polar molecules. After data filtering, 95 compounds were found in CHCl₃ fraction and 140 in MeOH fraction. The metabolites diversity indexes for these 2 fractions are presented in the Fig.2. In the CHCl₃ fraction containing the polar lipids (mainly in membranes, ie. phospholipids), the diversity of compounds was similar in D and HL conditions, while it decreased significantly between the D and ML following the light gradient. The chemical MeOH fraction contains the apolar lipids (also named neutral lipids, ie. triglycerides) and mid-polar compounds (ie. monosaccharids). The chemical diversity in the latter was higher than in the CHCl₃ fraction and tended to increase following the light gradient but without statistic significance (*Van der Waerden test* $p > 0.05$). Metabolomic fingerprints (pigment and detected metabolites) are presented in the BC-MFA (Fig.2). The light irradiance levels explained 44% of the total data variability (total inertia). The axis 1 discriminated the HL from the LL and ML conditions and the light irradiance gradient was conserved along axis 2. However, the D conditions are close to the 1000 $\mu\text{mol m}^{-2} \text{s}^{-1}$ conditions, showing that the biofilm could engage in similar metabolic responses when light-deprived or under too strong irradiances. The BC-MFA analysis permitted to highlight the compounds that significantly affected by the light irradiances. They were annotated and gathered in the table 2.

The samples exposed to HL and D were essentially characterized by compounds from the CHCl₃ fraction (Fig. 2, Fig. 3 and Fig.4). The PUFAs 7,10,13-Hexadecatrienoic acid (C16:3n-3; C111), 4,7,10,13,16,19-Docosahexaenoic acid (C22:6n-3, DHA; C178) and 7,10,13,16,19-Docosapentaenoic acid (22:5n-3, DPA; M306) were significantly more abundant in HL than in LL and ML (ANOVA, $p < 0.05$). The (E)-octadec-9-enoic acid (18:1n-9) is commonly measured in Chlorophyceae (Wiltshire, 2000), cyanobacteria (Abed et al., 2008) and bacteria (Véra et al., 2001). This FA was also suggested as characteristic of zooplankton and benthic metazoan (Kharlamenko et al., 2001; Nyssen et al., 2005; Zhukova and Kharlamenko, 1999) but is not systematically dominant in the benthic meiofauna such as in nematods (Leduc, 2008). The 16-methylheptadecanoic acid (iso-18:0; C141) and the heptadecanoic acid (C17:0; 146) values were also significantly higher under the HL and D than in LL and ML. The odd carbon chains and iso-branched SFAs are characteristic of heterotrophic bacteria (Dalsgaard et al., 2003; Kelly and Scheibling, 2012). The 9,10,12-trihydroxyoctadecanoic acid (C183) is a 3-hydroxy fatty acid (3-OHFA) derivative from the C18:0 FA. Because the 3-OHFAs are bonded to lipid A found in lipopolysaccharides and endotoxins of the gram-negative bacteria, these compounds are used as bacterial markers in dust (Hong et al., 2023), but 3-OHFAs from C18:0 were also measured in extracellular glycolipids of two fungi strains *Rhodotorula graminis* and

Rhodotorula glutinis (Stodola et al., 1967). The 3-OHFAs belong to the compounds group called oxylipins. Many of the latter are known to be intra and inter-specific signaling molecules allowing inter-Kingdom chemical communication between life forms (Pohl and Kock, 2014). The trihydroxyoctadecenoic acids are also suspected to have antibacterial properties like many hydroxylated FAs (Kim and Oh, 2013).

The tetradecane (C6), hexadecane (C23), hexadecane,2-methyl (C26), pristane (C28), nonadecane (C96) and 2-methyltricosane (C174) belong to the chemical family of alkanes. The alkene 5-octadecene (E) (C108), undetermined alkane (C19, C41, C50, C110 and C156) and neophytadiene (C70 and M194) were also produced in significantly higher proportion in HL and D than in the LL and ML conditions (Fig. 4, ANOVA and Van der Waerden test, $p < 0.05$). The pristane can be formed by biotic and abiotic degradation pathways. It can be synthesized by anaerobic bacteria through the oxidation of chlorophyll phytyl side-chain or trimeric α -tocopherol originating from senescent phytoplanktonic cells (Nassiry et al., 2009; Rontani et al., 2010). The zooplankton grazing activity was also found to be one important contributor to pristane amounts (Blumer and Snyder, 1965). The significantly higher value of pristane in biofilm under HL and D (ANOVA, $p < 0.05$) could be thus linked to MPB organisms' damage, and/or to a higher grazing activity of micro-meiofaunal organisms caused by the stressing irradiance conditions (darkness or too much light). The neophytadiene was measured in some microalgae (López-Rosales et al., 2019) like marine diatoms (Marella et al., 2021). This is an isoprenoid belonging to the terpene and it can arise from the phytol which is itself a *Chla* degradation product (Rontani and Volkman, 2003). It was reported as antimicrobial (Ahn et al., 2016). The tetradecane and nonadecane measured in methanol extract of cultured marine microalgae *Picochlorum* sp. RCC486 were also reported as antimicrobial and antioxidant compounds (Banakar and Jayaraj, 2018; Faridha Begum et al., 2016; Safavi et al., 2021). The nonadecane was one of the main hydrocarbons produced by the diatom *P.tricornum* and its accumulation under dark and HL could be attributed to the diatom's compartment of the biofilm (Dodson and Leblond, 2015). The 2-methyltricosane and the hexadecane,2-methyl are mono-branched alkanes reported to be abundant in cyanobacteria (Köster et al., 1999; Shiea et al., 1990) and proposed as a biomarker of this group (Robinson and Eglinton, 1990).

A majority of FAs and alka(e)nes characteristic of the light-stressing conditions appear to have bacterial origin. Neither the pigment analysis (table S2) nor the microscope observation (authors' observation) showed any substantial presence of cyanobacteria in the MPB presently studied. Furthermore, the metabolic variation was expected to be due to the responses of diatoms, since they were the photosynthetic microorganisms dominating the communities. MPB biofilms are a complex consortium of microorganisms whose interactions make it difficult to elucidate the origin of these metabolites. Hypotheses about the possible origins and roles of these lipids will be discussed further in this text, especially regarding the phototrophic and heterotrophic compartments of the biofilm.

The presence of alka(e)nes has been often measured in photosynthetic microorganisms, but their physiological functions remain poorly known (Schirmer et al., 2010; Solène L.Y. et al., 2021; Sorigué et al., 2016). In cyanobacteria, they are suspected to play a role in cell's growth and division, photosynthesis and salt tolerance (Berla et al., 2015; Koot and Pakrasi, 2019; Lea-Smith et al., 2016; Yamamori et al., 2018), and their presence in the thylakoïd membranes also regulates the redox balance under stress (Berla et al., 2015). In microalgae, they could also have such roles, but they remain poorly investigated and thus not understood. In the marine diatom *Rhizosolenia setigera*, the alkenes were suspected to play a role in their buoyancy and vertical migration (Sinninghe Damsté et al., 2000). The tetradecane and nonadecane were reported to have antioxidant properties (Banakar and Jayaraj, 2018; Faridha Begum et al., 2016; Safavi et al., 2021). In terrestrial plants and macroalgae, alka(e)nes are major constituents of waxes. They are known to protect them from stressing environmental conditions such as high light irradiances and ultraviolet exposures (Dominguez et al., 2011; Lee and Suh, 2015; Manning, 2022; Niklas et al., 2017; Yeats and Rose, 2013). Moreover, the latter were shown to induce an increase of the branched-chain alkanes content in plants' waxes (Barnes et al., 1994).

Whereas it has not been investigated yet on marine microalgae, the alka(e)nes synthesized by photosynthetic microorganisms probably also have similar photoprotective properties. In microalgae and various algal genera (*Nannochloropsis*, *Ectocarpus*, *Galdieria*, *Chondrus*), C15–C17 n-alkanes biosynthesis is presumed to be linked to photosynthetic membranes where they are biosynthesized from fatty acids (FAs) by decarboxylation of the corresponding aldehydes (Herman and Zhang, 2016; Sorigué et al., 2016). This decarboxylation can be catalyzed by the recently described photoenzyme named fatty acid photodecarboxylase (FAP), involving photons at each catalytic cycle (Solène L.Y. et al., 2021; Sorigué et al., 2017). Thus, the significant increase of alka(e)nes, in the HL conditions could be linked to a higher FAP activity in the biofilm microalgae. The high values of alka(e)nes measured in the dark conditions are not linked with the photon fluxes and thus cannot be attributed to the FAP activity but rather to non-light-dependent pathways. An accumulation of alkanes was also observed in a strain of the marine phytoplankton *Dicrateria rotunda* under dark conditions (Harada et al., 2021). But their synthesis in the dark conditions does not disprove the possibility that FAP and non-light-dependent mechanisms could work simultaneously under HL irradiances. The biofilm's accumulation of alka(e)nes could partly originate from MPB's organisms under both stressing dark and HL conditions. These hydrocarbons are part of FA metabolisms. Lipids and FA compositions of marine diatoms (Cointet et al., 2019; Duarte et al., 2021) are known to play a role in their adaption under light-induced stress. Notably, they change the membranes' characteristics with the increase in unsaturation of membrane lipids (Singh et al., 2002) allowing the solubilization of Dd essential for its de-epoxidation into Dt (Goss et al., 2007, 2005). The alka(e)nes may also be part of such mechanisms. Moreover, neutral lipids, such as hydrocarbons, are suspected to play a role in the long-term survival of microalgae under suboptimal conditions (Hu et al., 2008; Ramachandra et al., 2009).

Table.2 Annotated compounds identified with the BC-MFA analysis to vary under light irradiance levels

Comp.	Cos	Rmatch	CAS	Formula	Molecular name	Pathway	RIlit	RIexp
BC-MFA dimension 1								
M111	0.64	916	1731-88-0	C14H28O2	Tridecanoic acid	Fatty acids	1624	1608
M189	0.34	847	7132-64-1	C15H30O2	Pentadecanoic acid	Fatty acids	1820	1807
M306	0.05	775	108698-02-8	C23H36O2	(all Z)-7,10,13,16,19-Docosapentaenoic acid methyl ester	Fatty acids	NA	2040
C1	0.54	914	5779-94-2	C9H10O	Benzaldehyde, 2,5-dimethyl-	Terpenoids	1208	NA
C4	0.59	NA	NA	NA	NA	NA	NA	NA
C16	0.57	821	23676-09-7	C11H14O3	Benzoic acid, 4-ethoxy-, ethyl ester	Shikimates and Phenylpropanoids	1522	1518
C21	0.65	878	112-70-9	C13H28O	n-Tridecan-1-ol	Fatty acids	1577	1575
C23	0.53	904	544-76-3	C16H34	Hexadecane	Fatty acids	1600	1582
C24	0.95	840	638-53-9	C13H26O2	Tridecanoic acid	Fatty acids	1624	1603
C26	0.62	814	1560-92-5	C17H36	Hexadecane, 2-methyl-	Fatty acids	1664	1667
C28	0.75	NA	NA	NA	Pristane	Fatty acids	NA	1676
C36	0.84	928	544-63-8	C14H28O2	Tetradecanoic acid	Fatty acids	1725	1701
C41	0.44	NA	NA	NA	NA-alkane	Fatty acids	NA	1732
C50	0.59	NA	NA	NA	NA-alkane	Fatty acids	NA	1768
C51	0.55	NA	NA	NA	NA	NA	NA	1768
C54	0.6	NA	NA	NA	NA	NA	NA	1768
C56	0.73	738	544-64-9	C14H26O2	Myristoleic acid	Fatty acids	1783	1780
C57	0.7	635	5129-66-8	C15H30O2	Tetradecanoic acid, 12-methyl-	Fatty acids	1788	1780
C59	0.91	917	1002-84-2	C15H30O2	Pentadecanoic acid	Fatty acids	1820	1800
C60	0.92	727	6053-49-2	C16H30O2	Cyclopentaneundecanoic acid	Fatty acids	NA	1800
C70	0.46	895	504-96-1	C20H38	Neophytadiene	Terpenoids	1837	1840
C89	0.17	870	2271-34-3	C16H30O2	11E-hexadecenoic acid	NA	1886	1888
C96	0.27	718	629-92-5	C19H40	Nonadecane	NA	1900	1900
C108	0.74	885	7206-21-5	C18H36	5-Octadecene, (E)-	Fatty acids	NA	1969
C110	0.58	NA	NA	NA	Unknown Alkane	Fatty acids	NA	1969
C111	0.38	744	7561-64-0	C16H26O2	7,10,13-Hexadecatrienoic acid, (Z,Z,Z)-	Fatty acids	1945	1965
C114	0.52	900	NA	C18H34O2	(Z)-9-Heptadecenoic acid	NA	1989	1982
C125	0.62	NA	NA	NA	NA	Fatty acids	NA	2013
C141	0.5	816	2724-58-5	C19H38O2	16-methyl-heptadecanoic acid	NA	NA	2096
C146	0.48	615	14010-23-2	C17H38O2	Heptadecanoic acid	NA	2094	2096
C149	0.56	NA	NA	NA	NA	NA	NA	2140
C150	0.64	NA	NA	NA	NA	NA	NA	2140
C156	0.59	NA	NA	NA	NA-alkane	Fatty acids	NA	2163
C174	0.59	772	1928-30-9	C24H50	Tricosane, 2-methyl-	Fatty acids	2363	2364
C183	0.5	715	25027-95-6	C18H36O5	9,10,12-trihydroxyoctadecanoic acid	NA	NA	2597
Dd	0.69				Diadinoxanthin			
Dn	0.67				Dinoxanthin			
F.like2	0.58				Fucoxanthin like 2			
BC-MFA dimension 2								
M194	0.15	940	504-96-1	C20H38	Neophytadiene	Terpenoids	1837	1820
M214	0.49	784	56683-54-6	C16H32O2	(Z)-Hexadec-11-en-1-ol	NA	1867	1864
M248	0.41	NA	NA	NA	NA	NA	NA	1915
M289	0.34	NA	NA	NA	Unknown sugar	Carbohydrates	NA	1997
M404	0.3	NA	NA	NA	Unknown sugar	Carbohydrates	NA	2589
M412	0.32	NA	NA	NA	Unknown sugar	Carbohydrates	NA	2679
M417	0.35	NA	NA	NA	Unknown sugar	Carbohydrates	NA	2787
C6	0.48	948	629-59-4	C14H30	Tetradecane	Fatty acids	1400	1378
C19	0.3	NA	NA	NA	NA-branched alkane	Fatty acids	NA	1522
C99	0.42	NA	20170-32-5	C17H26O3	3-(3,5-Di-tert-butyl-4-hydroxyphenyl)propionic acid	Fatty acids	NA	1929
C133	0.75	826	NA	NA	NA	NA	NA	2068
C137	0.32		112-79-8	C18H34O2	Elaidic acid	Fatty acids	2076	2075
C178	0.23	890	6217-54-5	C22H32O2	4,7,10,13,16,19-Docosahexaenoic acid, (all-Z)-	Fatty acids	2471	2431
Ca	0.36				Chlorophyll a			
Ca.allo	0.35				Chlorophyll a allomer			
Dt	0.36				Diatoxanthin			
F.like1	0.4				Fucoxanthin like 1			
F	0.3				Fucoxanthin			

For GC-MS data (C, CHCl3 fraction and M, MeOH fractions), annotation was done with NIST 2017 (comp, compound; RI, Kovats retention indices; exp, experimental; lit, literature).

The production of alka(e)nes by marine heterotrophic bacteria is well studied in the domains of biofuels and bioremediation (Brown et al., 2019). They are used as energy sources by a wide diversity of marine genera such as *Alcanivorax*, but they have no other known biological roles yet (Van Beilen and Funhoff, 2007). As for microalgae, they can be biosynthesized from FAs (Brittingham et al., 2017; Radwan and Sorkhoh, 1993) or they can be taken up from their environment.

Two fatty alcohols also varied significantly under light irradiances (Fig. 3, table 2). The values of 1-tridecanol (C21) were significantly higher in the 750 and 1000 PAR conditions compared to the LL and ML (table 2, ANOVA, $p < 0.001$). The fatty alcohol (Z)-hexadec-11-en-1-ol (M214) was also measured in significantly higher values in the 500 PAR conditions than in LL and ML conditions (table 2, Van der Waerden test, $p < 0.05$). Same as for FA, the marine bacteria are known to produce odd chains of fatty alcohols with branches (Roper, 2004), the latter are thus likely linked with the bacterial compartment of the biofilm. The fatty alcohols are part of the metabolic pathway concerning the alkanes and FAs since they can be formed from alkanes and be converted in FAs through oxidation processes (Ishige et al., 2003; Soltani et al., 2004). The significant increase of 1-tridecanol could thus be linked with the significant alkanes' accumulation and with the FA's metabolism in the biofilm.

Independently of the alka(e)nes' and fatty alcohols' biological origin (heterotrophic or phototrophic), they appeared to play an important role in the photoacclimation of the mudflat biofilm at cellular and probably extracellular level (Marty and Saliot, 1976). They also underline the tight metabolic interactions between MPB and heterotrophic bacteria.

Metabolic fingerprints highlight diatom-bacteria interactions in light acclimation processes

The LL and ML conditions were characterized by 10 FAs (Fig. 5). The tetradecanoic acid (14:0; C36) is usually abundant in diatoms where it can represent more than 15% of their total fatty acids (Leu et al., 2007; Renaud et al., 1999). The 11E-hexadecenoic acid (C16:1-n5; C89) is also found in significant amount in diatoms (Leu et al., 2007). The lower amount of these FAs in HL than in LL and ML can be linked to the diatom response to light-induced stress above 500 $\mu\text{mol. photons. m}^{-2}.\text{s}^{-1}$. The cyclopentaneundecanoic acid (C60) is found in different microorganism's extracts. It represented 0.69% in the diatom *Amphora coffeaeformis* (Hassan et al., 2021), 22.7% in the bacteria *Glutamicibacter mysorens* (Karthik et al., 2023), 5.9 % and 11.06 % in the cyanobacteria *Lyngbya* sp. (Prasannabalaji et al., 2017) and *Anabaena sphaerica* (Abd El-Aty et al., 2014) respectively. This compound was associated with antibacterial and antioxidant properties (A.O and Temikotan, 2021). The (Z)-9-Heptadecenoic acid (C17:1n-8; C114) is also not specific to a microorganism taxa and is known to have antifungal properties (Avis et al., 2000; Ray et al., 2010). The 12-methyltetradecanoic acid (*anteiso*-C15:0, 12-MTA; C57) and the pentadecanoic acid (C15:0; C59 and M189) were previously found by our research team in the same sampling location and by the same untargeted metabolomic analysis method (Gaubert-Boussarie et al., 2020). They are known as heterotrophic bacteria markers, usually composed by odd carbon chains, iso- and anteiso-branched SFA and MUFA [66, 67] where the *anteiso*-C15:0 is generally associated with the genus *Bacillus* (Kaneda, 1977; Ntougias et al., 2000). The myristoleic acid (C14:1n-5; C56), the *anteiso*-C15:0 and other branched-chain FAs are known to have antibacterial properties (Inoue et al., 2008; Kumar et al., 2020).

In this work, the LL and ML conditions showed low DES values and they are in the range of optimal light levels for benthic diatoms (Ezequiel et al., 2015; Prella and Karsten, 2022). The metabolites present in these

conditions corresponded thus to a biofilm with photosynthetic organisms in an optimal physiological state. Interestingly, saturated and monounsaturated fatty acids (SFAs and MUFAs) dominated the FAs in these photosynthetic optimal conditions while PUFAs were characteristic of light stressing conditions (Fig.3 and Fig.5). The photon flux density was shown to trigger an accumulation of FAs in microalgae (Piepho et al., 2012; Wainman et al., 1999; Wang et al., 2015) and was suggest to contribute to higher FAs content in the all microphytobenthic biofilm during spring compared to winter (Schnurr et al., 2019). This is consistent with the higher values of tetradecanoic acid and 11E-hexadecenoic acid related to the diatoms under LL and ML than in the dark conditions. On the contrary, stressing conditions such as nutrient depletion was observed to generate in diatoms an FAs accumulation by reallocating carbon from growth to storage (Grosse et al., 2018; Mus et al., 2013; Schnurr et al., 2013). The great values of DHA observed under D and HL could be thus linked with light-stress induced by these conditions.

Although the diatoms dominate the MPB, excepted the 3 latter FAs described above, most of the measured compounds associated with FAs' metabolism varying under light irradiance levels seemed to have bacterial origin. Because the desaturation of SFA and MUFA requires large amounts of NAD(P)H and oxygen, it was proposed that the PUFAs' synthesis could contribute to the reactive oxygen species scavenging in microorganisms' cells when they are under stressing conditions (Arora et al., 2019; Patel et al., 2016). On the one hand, the high proportion of PUFAs under HL may thus be triggered in response to the light-stressing conditions. On the other hand, the increase of SFAs, MUFAs and branched FAs under LL and ML could be attributed to the phototrophic bacteria or to heterotrophic bacteria in tight biological interaction with the autotrophic organisms. Depending on the species, benthic diatoms can have different associated bacteria (Behringer et al., 2018; Doiron et al., 2012; Schäfer et al., 2002). In intertidal mudflat biofilms, MPB and bacteria communities' composition were observed to co-variate, enlightening this strong biological interaction *in situ* (Bolhuis et al., 2013; Decleyre et al., 2015; Lavergne et al., 2017). Benthic diatoms were observed to promote or disadvantage bacteria strains notably through the production of exopolymers (Doghri et al., 2017).

Under HL irradiances, the MPB organisms migrated downward the sediment (visual observation). In a study comparing the vertical migration kinetics of mudflat MPB under the same light irradiances as the present study (50, 100, 250, 500, 1000 and 1350 $\mu\text{mol photons m}^{-2} \text{s}^{-1}$), the intensity of the light-induced migratory response varied nonlinearly with the irradiance levels (Laviale et al., 2016). Interestingly, the diatoms' biomass variation at the sediment surface as a function of the different irradiance's levels followed the same pattern as the metabolic fingerprint found in the present study. An upward migration was induced below 250 $\mu\text{mol photons m}^{-2} \text{s}^{-1}$. Above this light threshold, MPB moved downward with more pronounced speed and depth at 1000 than in 500 $\mu\text{mol photons m}^{-2} \text{s}^{-1}$. During the light exposure, we could not follow the vertical migration by fluorescence measurements, but this suggests that the metabolic biofilm's responses to the light irradiance levels could be tightly linked with the MPB migratory photoresponse. In

diatoms, the vertical migration is realized by the excretion of more EPS, notably exopolysaccharides. The latter are sugar polymers known to serve as food sources for many biofilm bacteria (King, 1986; Van Duyl et al., 1999). The increase and the qualitative changes of extracellular polymeric substances (EPS) production during the vertical migration could have induced important changes of bacterial metabolisms while it protected the diatoms from HL irradiance damage. The significant variations of the unidentified sugars amounts (M289, M404, M412, M417, table 2) under the light irradiances are consistent with this hypothesis. Moreover, the 1000 $\mu\text{mol photons m}^{-2} \text{s}^{-1}$ could trigger a deeper downward migration into the sediment than the 500 and 700 $\mu\text{mol photons m}^{-2} \text{s}^{-1}$ PAR irradiances, placing the migrating MPB organisms closer to darkness conditions. A deeper migration under 1000 $\mu\text{mol photons m}^{-2} \text{s}^{-1}$ PAR than in the other HL conditions could thus partly explain the similarity of MPB metabolic fingerprints between this irradiance level and the dark conditions.

Conclusion

To our knowledge, it is the first time that an untargeted metabolomic analysis was applied on mudflat biofilm to investigate its global metabolic response to a light gradient. This method allowed to identify metabolites involved in two types of responses to light irradiances. The production of diatoms and bacterial origin FAs corresponding to good photosynthesis state of MPB under LL and ML, enlightened the tight interactions between the prokaryotic and phototropic compartment of the biofilm. Alka(e)nes and fatty alcohols, both derived from FA's metabolisms, were produced under dark and light-induced stress triggered by HL. The physiological and ecological functions of these compounds are poorly described in literature. Alka(e)nes can be synthesized by both autotrophic and heterotrophic microorganisms, but also taken up and metabolized by the latter. Surprisingly, the compounds observed to vary significantly were mostly linked with the bacteria compartment of the biofilm. To our knowledge, the interactions diatoms-bacteria have never been explored in the context of photoacclimation, and it would be interesting to lead investigations in this way. Moreover, independently of their biological origin, alka(e)nes and fatty alcohols appeared to play important unexplored roles in dark and light-induced stress acclimation of MPB biofilms. Their implications in stress responses deserve deeper research and could be investigated through targeted approaches on hydrocarbons. The significant increase of the 3-OHFA under D and HL in the biofilm suggest that the oxylipins could play a role in the signal of the light induce stress responses. In general, the present study underlined the importance of FAs metabolism in the mudflat biofilm responses to light. The untargeted method applied on MPB biofilm under a gradient of light representative of natural irradiances brought out interesting research avenues to better understand the chemical ecology of such complex communities.

Acknowledgments

This study was funded by the Regional Council of French Brittany, the General Council of Finistère. The authors would like to thank two anonymous reviewers for their valuable comments, which greatly

contributed to the improvement of this article. D.C. acknowledges the language assistance received from Marius Bunner.

References

- A.O, D., Temikotan, T., 2021. Fatty acid profile, antioxidant and antibacterial effect of the ethyl acetate extract of *Cleistopholis patens*. Bull. Sci. Res. 21–31. <https://doi.org/10.34256/bsr2113>
- Abd El-Aty, A.M., Mohamed, A.A., Samhan, F.A., 2014. In vitro antioxidant and antibacterial activities of two fresh water Cyanobacterial species, *Oscillatoria agardhii* and *Anabaena sphaerica*. J. Appl. Pharm. Sci. 4, 69–75. <https://doi.org/10.7324/JAPS.2014.40712>
- Abed, R.M.M., Kohls, K., Schoon, R., Scherf, A.K., Schacht, M., Palinska, K.A., Al-Hassani, H., Hamza, W., Rullkötter, J., Golubic, S., 2008. Lipid biomarkers, pigments and cyanobacterial diversity of microbial mats across intertidal flats of the arid coast of the Arabian Gulf (Abu Dhabi, UAE). FEMS Microbiol. Ecol. 65, 449–462. <https://doi.org/10.1111/j.1574-6941.2008.00537.x>
- Ahn, H.M., Kim, S.-H., Hyun, S.-H., Lim, S.R., Kim, H.-Y., Oh, J., Lee, K.-M., Hong, S.-J., Cho, B.-K., Lee, H., Lee, C.-G., Choi, H.-K., 2016. Effects of the timing of a culture temperature reduction on the comprehensive metabolite profiles of *Chlorella vulgaris*. J. Appl. Phycol. 28, 2641–2650. <https://doi.org/10.1007/s10811-016-0817-4>
- Arora, N., Patel, A., Mehtani, J., Pruthi, P.A., Pruthi, V., Poluri, K.M., 2019. Co-culturing of oleaginous microalgae and yeast: paradigm shift towards enhanced lipid productivity. Environ. Sci. Pollut. Res. 26, 16952–16973. <https://doi.org/10.1007/s11356-019-05138-6>
- Avis, T.J., Boulanger, R.R., Bélanger, R.R., 2000. Synthesis and biological characterization of (Z)-9-heptadecenoic and (Z)-6-methyl-9-heptadecenoic acids: Fatty acids with antibiotic activity produced by *Pseudozyma flocculosa*. J. Chem. Ecol. 26, 987–1000. <https://doi.org/10.1023/A:1005464326573>
- Banakar, P., Jayaraj, M., 2018. Gc-MS analysis of bioactive compounds from ethanolic leaf extract of *Waltheria indica* Linn. and their pharmacological activities. Int. J. Pharm. Sci. Res. 9, 2005–2010. [https://doi.org/10.13040/IJPSR.0975-8232.9\(5\).2005-10](https://doi.org/10.13040/IJPSR.0975-8232.9(5).2005-10)
- Barnes, J., Paul, N., Percy, K., Broadbent, P., McLaughlin, C., Mullineaux, P., Creissen, G., Wellburn, A., 1994. Effects of UV-B radiation on wax biosynthesis, in: Air Pollutants and the Leaf Cuticle. Springer, Berlin, Heidelberg, pp. 195–204. https://doi.org/10.1007/978-3-642-79081-2_16
- Barnett, A., Méléder, V., Dupuy, C., Lavaud, J., 2020. The vertical migratory rhythm of intertidal microphytobenthos in sediment depends on the light photoperiod, intensity, and spectrum: evidence for a positive effect of blue wavelengths. Front. Mar. Sci. 7, 1–18. <https://doi.org/10.3389/fmars.2020.00212>
- Behringer, G., Ochsenkühn, M.A., Fei, C., Fanning, J., Koester, J.A., Amin, S.A., 2018. Bacterial communities of diatoms display strong conservation across strains and time. Front. Microbiol. 9, 1–15. <https://doi.org/10.3389/FMICB.2018.00659>
- Beninger, P.G., Paterson, D.M., 2018. Mudflat Ecology, Aquatic Ec. ed. Springer Nature. <https://doi.org/10.1007/978-3-319-99194-8>
- Berla, B.M., Saha, R., Maranas, C.D., Pakrasi, H.B., 2015. Cyanobacterial alkanes modulate photosynthetic cyclic electron flow to assist growth under cold stress. Sci. Rep. 5, 1–12. <https://doi.org/10.1038/srep14894>

- Blanchard, G.F., Guarini, J.M., Dang, C., Richard, P., 2004. Characterizing and quantifying photoinhibition in intertidal microphytobenthos. *J. Phycol.* 40, 692–696. <https://doi.org/10.1111/j.1529-8817.2004.03063.x>
- Blumer, M., Snyder, W.D., 1965. Isoprenoid hydrocarbons in recent sediments: presence of pristane and probable absence of phytane. *Science* (80-). 150, 1588–1589.
- Bolhuis, H., Fillinger, L., Stal, L.J., 2013. Coastal microbial mat diversity along a natural salinity gradient. *PLoS One* 8, 1–12. <https://doi.org/10.1371/JOURNAL.PONE.0063166>
- Brittingham, A., Hren, M.T., Hartman, G., 2017. Microbial alteration of the hydrogen and carbon isotopic composition of n-alkanes in sediments. *Org. Geochem.* 107, 1–8. <https://doi.org/10.1016/j.orggeochem.2017.01.010>
- Brotas, V., Plante-Cuny, M.R., 2003. The use of HPLC pigment analysis to study microphytobenthos communities, in: *Acta Oecologica*. Elsevier, pp. 109–115. [https://doi.org/10.1016/S1146-609X\(03\)00013-4](https://doi.org/10.1016/S1146-609X(03)00013-4)
- Brown, S., Loh, J., Aves, S.J., Howard, T.P., 2019. Alkane biosynthesis in bacteria, in: *Biogenesis of Hydrocarbons*. Springer, Cham, pp. 451–470. https://doi.org/10.1007/978-3-319-78108-2_7
- Bundy, J.G., Matthew, A.E., Davey, P., Viant, M.R., 2009. Environmental metabolomics: a critical review and future perspectives. *Metabolomics* 3–21. <https://doi.org/10.1007/s11306-008-0152-0>
- Cartaxana, P., Ruivo, M., Hubas, C., Davidson, I., Serôdio, J., Jesus, B., 2011. Physiological versus behavioral photoprotection in intertidal epipellic and epipsammic benthic diatom communities. *J. Exp. Mar. Bio. Ecol.* 405, 120–127. <https://doi.org/10.1016/J.JEMBE.2011.05.027>
- Chambers, M.C., MacLean, B., Burke, R., Amodei, D., Ruderman, D.L., Neumann, S., Gatto, L., Fischer, B., Pratt, B., Egertson, J., Hoff, K., Kessner, D., Tasman, N., Shulman, N., Frewen, B., Baker, T.A., Brusniak, M.Y., Paulse, C., Creasy, D., Flashner, L., Kani, K., Moulding, C., Seymour, S.L., Nuwaysir, L.M., Lefebvre, B., Kuhlmann, F., Roark, J., Rainer, P., Detlev, S., Hemenway, T., Huhmer, A., Langridge, J., Connolly, B., Chadick, T., Holly, K., Eckels, J., Deutsch, E.W., Moritz, R.L., Katz, J.E., Agus, D.B., MacCoss, M., Tabb, D.L., Mallick, P., 2012. A cross-platform toolkit for mass spectrometry and proteomics. *Nat. Biotechnol.* 2012 3010 30, 918–920. <https://doi.org/10.1038/nbt.2377>
- Chevalier, E.M., Gévaert, F., Créach, A., 2010. In situ photosynthetic activity and xanthophylls cycle development of undisturbed microphytobenthos in an intertidal mudflat. *J. Exp. Mar. Bio. Ecol.* 385, 44–49. <https://doi.org/10.1016/j.jembe.2010.02.002>
- Coelho, H., Vieira, S., Serôdio, J., 2011. Endogenous versus environmental control of vertical migration by intertidal benthic microalgae. *Eur. J. Phycol.* 46, 271–281. <https://doi.org/10.1080/09670262.2011.598242>
- Cointet, E., Wielgosz-Collin, G., Bougaran, G., Rabesaotra, V., Gonçalves, O., Méléder, V., 2019. Effects of light and nitrogen availability on photosynthetic efficiency and fatty acid content of three original benthic diatom strains. *PLoS One* 14, 1–28. <https://doi.org/10.1371/JOURNAL.PONE.0224701>
- Consalvey, M., Paterson, D.M., Underwood, G.J.C., 2004. The ups and downs of life in a benthic biofilm: Migration of benthic diatoms. *Diatom Res.* 19, 181–202. <https://doi.org/10.1080/0269249X.2004.9705870>

- Cruz, S., Serôdio, J., 2008. Relationship of rapid light curves of variable fluorescence to photoacclimation and non-photochemical quenching in a benthic diatom. *Aquat. Bot.* 88, 256–264. <https://doi.org/10.1016/j.aquabot.2007.11.001>
- Dalsgaard, J., St. John, M., Kattner, G., Müller-Navarra, D., Hagen, W., 2003. Fatty acid trophic markers in the pelagic marine environment. *Adv. Mar. Biol.* 46, 225–340. [https://doi.org/10.1016/S0065-2881\(03\)46005-7](https://doi.org/10.1016/S0065-2881(03)46005-7)
- Decleyre, H., Heylen, K., Sabbe, K., Tytgat, B., Deforce, D., Van Nieuwerburgh, F., Van Colen, C., Willems, A., 2015. A Doubling of microphytobenthos biomass coincides with a tenfold Increase in denitrifier and total bacterial abundances in intertidal sediments of a temperate estuary. *PLoS One* 10, 1–23. <https://doi.org/10.1371/JOURNAL.PONE.0126583>
- Dodson, V.J., Leblond, J.D., 2015. Now you see it, now you don't: differences in hydrocarbon production in the diatom *Phaeodactylum tricornutum* due to growth temperature. *J. Appl. Phycol.* 27, 1463–1472. <https://doi.org/10.1007/S10811-014-0464-6/FIGURES/2>
- Doghri, I., Lavaud, J., Dufour, A., Bazire, A., Lanneluc, I., Sablé, S., 2017. Cell-bound exopolysaccharides from an axenic culture of the intertidal mudflat *Navicula phyllepta* diatom affect biofilm formation by benthic bacteria. *J. Appl. Phycol.* 29, 165–177. <https://doi.org/10.1007/s10811-016-0943-z>
- Doiron, K., Linossier, I., Fay, F., Yong, J., Abd Wahid, E., Hadjiev, D., Bourgougnon, N., 2012. Dynamic approaches of mixed species biofilm formation using modern technologies. *Mar. Environ. Res.* 78, 40–47. <https://doi.org/10.1016/J.MARENRES.2012.04.001>
- Domingo-Almenara, X., Brezmes, J., Vinaixa, M., Samino, S., Ramirez, N., Ramon-Krauel, M., Lerin, C., Díaz, M., Ibáñez, L., Correig, X., Perera-Lluna, A., Yanes, O., 2016. ERah: A computational tool integrating spectral deconvolution and alignment with quantification and identification of metabolites in GC/MS-based metabolomics. *Anal. Chem.* 88, 9821–9829. <https://doi.org/10.1021/acs.analchem.6b02927>
- Dominguez, E., Heredia-Guerrero, J.A., Heredia, A., 2011. The biophysical design of plant cuticles: an overview. *New Phytol.* 189, 938–949. <https://doi.org/10.1111/J.1469-8137.2010.03553.X>
- Dove, A.D.M., Leisen, J., Zhou, M., Byrne, J.J., Lim-Hing, K., Webb, H.D., Gelbaum, L., Viant, M.R., Kubanek, J., Fernández, F.M., 2012. Biomarkers of whale shark health: a metabolomic approach. *PLoS One* 7, e49379. <https://doi.org/10.1371/JOURNAL.PONE.0049379>
- Du, G., Yan, H., Liu, C., Mao, Y., 2018. Behavioral and physiological photoresponses to light intensity by intertidal microphytobenthos. *J. Oceanol. Limnol.* 36, 293–304. <https://doi.org/10.1007/s00343-017-6099-0>
- Du, G.Y., Oak, J.-H., Li, H., Chung, I.-K., 2010. Effect of light and sediment grain size on the vertical migration of benthic diatoms. *Algae* 25, 133–140. <https://doi.org/10.4490/algae.2010.25.3.133>
- Duarte, B., Feijão, E., Goessling, J.W., Caçador, I., Matos, A.R., 2021. Pigment and fatty acid production under different light qualities in the diatom *Phaeodactylum tricornutum*. *Appl. Sci.* 2021, Vol. 11, Page 2550 11, 2550. <https://doi.org/10.3390/APP11062550>
- Elias, S., Banin, E., 2012. Multi-species biofilms: living with friendly neighbors. *FEMS Microbiol. Rev.* 36, 990–1004. <https://doi.org/10.1111/J.1574-6976.2012.00325.X>

- Ezequiel, J., Laviale, M., Frankenbach, S., Cartaxana, P., SerÔdio, J., 2015. Photoacclimation state determines the photobehaviour of motile microalgae: The case of a benthic diatom. *J. Exp. Mar. Bio. Ecol.* 468, 11–20. <https://doi.org/10.1016/j.jembe.2015.03.004>
- Faridha Begum, I., Mohankumar, R., Jeevan, M., Ramani, K., 2016. GC–MS analysis of bio-active molecules derived from *Paracoccus pantotrophus* FMR19 and the antimicrobial activity against bacterial pathogens and MDROs. *Indian J. Microbiol.* 56, 426. <https://doi.org/10.1007/S12088-016-0609-1>
- Flemming, H.C., Wingender, J., 2010. The biofilm matrix. *Nat. Rev. Microbiol.* 8, 623–633. <https://doi.org/10.1038/nrmicro2415>
- Gaillard, F., Potin, P., 2014. Proteomics and metabolomics of marine organisms: Current strategies and knowledge, in: La Barre, S., Kornprobst, J.-M. (Eds.), *Outstanding Marine Molecules: Chemistry, Biology, Analysis*. pp. 457–472.
- Gaubert-Boussarie, J., Prado, S., Hubas, C., 2020. An untargeted metabolomic approach for microphytobenthic biofilms in intertidal mudflats. *Front. Mar. Sci.* 7, 250. <https://doi.org/10.3389/fmars.2020.00250>
- Goss, R., Jakob, T., 2010. Regulation and function of xanthophyll cycle-dependent photoprotection in algae. *Photosynth. Res.* 106, 103–122. <https://doi.org/10.1007/S11120-010-9536-X>
- Goss, R., Latowski, D., Grzyb, J., Vieler, A., Lohr, M., Wilhelm, C., Strzalka, K., 2007. Lipid dependence of diadinoxanthin solubilization and de-epoxidation in artificial membrane systems resembling the lipid composition of the natural thylakoid membrane. *Biochim. Biophys. Acta - Biomembr.* 1768, 67–75. <https://doi.org/10.1016/J.BBAMEM.2006.06.006>
- Goss, R., Lepetit, B., 2015. Biodiversity of NPQ. *J. Plant Physiol.* 172, 13–32. <https://doi.org/10.1016/J.JPLPH.2014.03.004>
- Goss, R., Lohr, M., Latowski, D., Grzyb, J., Vieler, A., Wilhelm, C., Strzalka, K., 2005. Role of hexagonal structure-forming lipids in diadinoxanthin and violaxanthin solubilization and de-epoxidation. *Biochemistry* 44, 4028–4036. <https://doi.org/10.1021/BI047464K>
- Grosse, J., Brussaard, C.P.D., Boschker, H.T.S., 2018. Nutrient limitation driven dynamics of amino acids and fatty acids in coastal phytoplankton. *Limnol. Oceanogr.* 64, 302–316. <https://doi.org/10.1002/Lno.11040>
- Harada, N., Hirose, Y., Chihong, S., Kurita, H., Sato, M., Onodera, J., Murata, K., Itoh, F., 2021. A novel characteristic of a phytoplankton as a potential source of straight-chain alkanes. *Sci. Reports* 2021 111 11, 1–12. <https://doi.org/10.1038/s41598-021-93204-w>
- Haro, S., Bohórquez, J., Lara, M., Garcia-Robledo, E., González, C.J., Crespo, J.M., Papaspyrou, S., Corzo, A., 2019. Diel patterns of microphytobenthic primary production in intertidal sediments: the role of photoperiod on the vertical migration circadian rhythm. *Sci. Rep.* 9, 1–10. <https://doi.org/10.1038/s41598-019-49971-8>
- Hassan, M.E., El-Sayed, A.E.K.B., Abdel-Wahhab, M.A., 2021. Screening of the bioactive compounds in *Ampora coffeaeformis* extract and evaluating its protective effects against deltamethrin toxicity in rats. *Environ. Sci. Pollut. Res.* 28, 15185–15195. <https://doi.org/10.1007/s11356-020-11745-5>
- Henley, W.J., 1993. Measurement and interpretation of photosynthetic light-Response curves in algae in the context of photoinhibition and diel changes. *J. Phycol.*

- Herlory, O., Richard, P., Blanchard, G.F., 2007. Methodology of light response curves: application of chlorophyll fluorescence to microphytobenthic biofilms. *Mar. Biol.* 153, 91–101. <https://doi.org/10.1007/S00227-007-0787-9>
- Herman, N.A., Zhang, W., 2016. Enzymes for fatty acid-based hydrocarbon biosynthesis. *Curr. Opin. Chem. Biol.* 35, 22–28. <https://doi.org/10.1016/j.cbpa.2016.08.009>
- Hong, G., Han, Y.K., Yeo, M.K., Lee, B.G., Na, Y.C., 2023. Development of analytical methods for the determination of 3-hydroxy fatty acids and muramic acid as bacterial markers in airborne particles and settled dust. *J. Chromatogr. A* 1688, 463708. <https://doi.org/10.1016/j.chroma.2022.463708>
- Hörnlein, C., Confurius-Guns, V., Grego, M., Stal, L.J., Bolhuis, H., 2020. Circadian clock-controlled gene expression in co-cultured, mat-forming cyanobacteria. *Sci. Rep.* 10, 1–17. <https://doi.org/10.1038/s41598-020-69294-3>
- Hu, Q., Sommerfeld, M., Jarvis, E., Ghirardi, M., Posewitz, M., Seibert, M., Darzins, A., 2008. Microalgal triacylglycerols as feedstocks for biofuel production: perspectives and advances. *plant J.* 54, 621–639. <https://doi.org/10.1111/j.1365-313X.2008.03492.x>
- Hubas, C., Passarelli, C., Paterson, D.M., 2018. Microphytobenthic biofilms: composition and interactions, in: Beninger, P.G. (Ed.), *Mudflat Ecology*. Springer Nature Switzerland, pp. 63–90. https://doi.org/10.1007/978-3-319-99194-8_4
- Inoue, T., Shingaki, R., Fukui, K., 2008. Inhibition of swarming motility of *Pseudomonas aeruginosa* by branched-chain fatty acids. *FEMS Microbiol. Lett.* 281, 81–86. <https://doi.org/10.1111/J.1574-6968.2008.01089.X>
- Ishige, T., Krause, M., Bott, M., Wendisch, V.F., Sahm, H., 2003. The phosphate starvation stimulon of *Corynebacterium glutamicum* determined by DNA microarray analyses. *J. Bacteriol.* 185, 4519. <https://doi.org/10.1128/JB.185.15.4519-4529.2003>
- Jesus, B., Perkins, R.G., Mendes, C.R., Brotas, V., Paterson, D.M., 2006. Chlorophyll fluorescence as a proxy for microphytobenthic biomass: alternatives to the current methodology. *Mar. Biol.* 17–28. <https://doi.org/10.1007/s00227-006-0324-2>
- Jordan, L., McMinn, A., Thompson, P., 2010. Diurnal changes of photoadaptive pigments in microphytobenthos. *J. Mar. Biol. Assoc. United Kingdom* 90, 1025–1032. <https://doi.org/10.1017/S0025315409990816>
- Jordan, L., McMinn, A., Wotherspoon, S., 2008. Diurnal and monthly vertical profiles of benthic microalgae within intertidal sediments from two temperate localities. *Mar. Freshw. Res.* 59, 931–939. <https://doi.org/10.1071/MF07105>
- Kaneda, T., 1977. Fatty acids of the genus *Bacillus*: an example of branched-chain preference. *Bacteriol. Rev.* 41, 391–418. <https://doi.org/10.1128/BR.41.2.391-418.1977>
- Karthik, Y., Ishwara Kalyani, M., Krishnappa, S., Devappa, R., Anjali Goud, C., Ramakrishna, K., Wani, M.A., Alkafafy, M., Hussien Abduljabbar, M., Alswat, A.S., Sayed, S.M., Mushtaq, M., 2023. Antiproliferative activity of antimicrobial peptides and bioactive compounds from the mangrove *Glutamicibacter myso-rens*. *Front. Microbiol.* 14. <https://doi.org/10.3389/fmicb.2023.1096826>

- Kelly, J.R., Scheibling, R.E., 2012. Fatty acids as dietary tracers in benthic food webs. *Mar. Ecol. Prog. Ser.* 446, 1–22. <https://doi.org/10.3354/meps09559>
- Kharlamenko, V.I., Kiyashko, S.I., Imbs, A.B., Vyshkvartzev, D.I., 2001. Identification of food sources of invertebrates from the seagrass *Zostera marina* community using carbon and sulfur stable isotope ratio and fatty acid analyses. *Mar. Ecol. Prog. Ser.* 220, 103–117. <https://doi.org/10.3354/meps220103>
- Kim, K., Oh, D., 2013. Production of hydroxy fatty acids by microbial fatty acid-hydroxylation enzymes. *Biotechnol. Adv.* 31, 1473–1485. <https://doi.org/10.1016/j.biotechadv.2013.07.004>
- King, G.M., 1986. Characterization of β -glucosidase activity in intertidal marine sediments. *Appl. Environ. Microbiol.* 51, 373–380. <https://doi.org/10.1128/aem.51.2.373-380.1986>
- Knoot, C.J., Pakrasi, H.B., 2019. Diverse hydrocarbon biosynthetic enzymes can substitute for olefin synthase in the cyanobacterium *Synechococcus* sp. PCC 7002. *Sci. Rep.* 9, 1360. <https://doi.org/10.1038/S41598-018-38124-Y>
- Köster, J., Volkman, J.K., Rullkötter, J., Scholz-Böttcher, B.M., Rethmeier, J., Fischer, U., 1999. Mono-, di- and trimethyl-branched alkanes in cultures of the filamentous cyanobacterium *Calothrix scopulorum*. *Org. Geochem.* 30, 1367–1379. [https://doi.org/10.1016/S0146-6380\(99\)00110-2](https://doi.org/10.1016/S0146-6380(99)00110-2)
- Kumar, P., Lee, J.H., Beyenal, H., Lee, J., 2020. Fatty acids as antibiofilm and antivirulence agents. *Trends Microbiol.* 28, 753–768. <https://doi.org/10.1016/j.tim.2020.03.014>
- Lavaud, J., 2007. Fast regulation of photosynthesis in diatoms: mechanisms, evolution and ecophysiology. *Funct. Plant Sci. Biotechnonology* 1, 267–287.
- Lavaud, J., Rousseau, B., Etienne, A.L., 2004. General features of photoprotection by energy dissipation in planktonic diatoms (Bacillariophyceae). *J. Phycol.* 40, 130–137. <https://doi.org/10.1046/J.1529-8817.2004.03026.X>
- Lavaud, J., Rousseau, B., Etienne, A.L., 2002. In diatoms, a transthylakoid proton gradient alone is not sufficient to induce a non-photochemical fluorescence quenching. *FEBS Lett.* 523, 163–166. [https://doi.org/10.1016/S0014-5793\(02\)02979-4](https://doi.org/10.1016/S0014-5793(02)02979-4)
- Lavergne, C., Agogué, H., Leynaert, A., Raimonet, M., De Wit, R., Pineau, P., Bréret, M., Lachaussée, N., Dupuy, C., 2017. Factors influencing prokaryotes in an intertidal mudflat and the resulting depth gradients. *Estuar. Coast. Shelf Sci.* 189, 74–83. <https://doi.org/10.1016/J.ECSS.2017.03.008>
- Laviale, M., Barnett, A., Ezequiel, J., Lepetit, B., Frankenbach, S., Méléder, V., Serôdio, J., Lavaud, J., 2015. Response of intertidal benthic microalgal biofilms to a coupled light–temperature stress: evidence for latitudinal adaptation along the Atlantic coast of Southern Europe. *Environ. Microbiol.* 17, 3662–3677. <https://doi.org/10.1111/1462-2920.12728>
- Laviale, M., Frankenbach, S., Serôdio, J., 2016. The importance of being fast: comparative kinetics of vertical migration and non-photochemical quenching of benthic diatoms under light stress. *Mar. Biol.* 163, 1–12. <https://doi.org/10.1007/s00227-015-2793-7>
- Lea-Smith, D.J., Ortiz-Suarez, M.L., Lenn, T., Nürnberg, D.J., Baers, L.L., Davey, M.P., Parolini, L., Huber, R.G., Cotton, C.A.R., Mastroianni, G., Bombelli, P., Ungerer, P., Stevens, T.J., Smith, A.G., Bond, P.J., Mullineaux, C.W., Howe, C.J., 2016. Hydrocarbons are essential for optimal cell size, division, and growth of cyanobacteria. *Plant Physiol.* 172, 1928–1940. <https://doi.org/10.1104/PP.16.01205>

- Leduc, D., 2008. Description of *Oncholaimus moanae* sp. nov. (Nematoda : Oncholaimidae), with notes on feeding ecology based on isotopic and fatty acid composition. *J. Mar. Biol. Assoc. UK* 89, 337–344. <https://doi.org/10.1017/S0025315408002464>
- Lee, S.B., Suh, M.C., 2015. Advances in the understanding of cuticular waxes in *Arabidopsis thaliana* and crop species. *Plant Cell Rep.* 34, 557–572. <https://doi.org/10.1007/S00299-015-1772-2/TABLES/3>
- Leu, E., Falk-Petersen, S., Hessen, D.O., 2007. Ultraviolet radiation negatively affects growth but not food quality of arctic diatoms. *Limnol. Oceanogr.* 52, 787–797. <https://doi.org/10.4319/LO.2007.52.2.0787>
- López-Rosales, A.R., Ancona-Canché, K., Carlos Chavarria-Hernandez, J., Barahona-Pérez, F., Toledano-Thompson, T., Garduño-Solórzano, G., López-Adrian, S., Canto-Canché, B., Polanco-Lugo, E., Valdez-Ojeda, R., 2019. Fatty acids, hydrocarbons and terpenes of *Nannochloropsis* and *Nannochloris* isolates with potential for biofuel production. *Energies* 12, 130. <https://doi.org/10.3390/en12010130>
- Macintyre, H.L., Geider, R.J., Miller, D.C., 1996. Microphytobenthos: The ecological role of the “secret garden” of unvegetated, shallow-water marine habitats. I. Role in sediment stability and shallow-water food webs. *Estuaries* 19, 202–212. <https://doi.org/10.2307/1352225>
- Maggi, E., Jackson, A.C., Tolhurst, T., Underwood, A.J., Chapman, M.G., 2013. Changes in microphytobenthos fluorescence over a tidal cycle: implications for sampling designs. *Hydrobiologia* 701, 301–312. <https://doi.org/10.1007/s10750-012-1291-x>
- Manning, S.R., 2022. Microalgal lipids: biochemistry and biotechnology. *Curr. Opin. Biotechnol.* 74, 1–7. <https://doi.org/10.1016/J.COPBIO.2021.10.018>
- Marella, T.K., Bansal, H., Bhattacharjya, R., Himanshu, Parmar, N., Chaurasia, A., Watanabe, M.M., Bhatnagar, A., Tiwari, A., 2021. Deciphering functional biomolecule potential of marine diatoms through complex network approach. *Bioresour. Technol.* 342, 125927. <https://doi.org/10.1016/J.BIORTECH.2021.125927>
- Marty, J.C., Saliot, A., 1976. Hydrocarbons (normal alkanes) in the surface microlayer of seawater. *Deep. Res. Oceanogr. Abstr.* 23, 863–873. [https://doi.org/10.1016/0011-7471\(76\)90853-6](https://doi.org/10.1016/0011-7471(76)90853-6)
- Mouget, J.L., Perkins, R., Consalvey, M., Lefebvre, S., 2008. Migration or photoacclimation to prevent high irradiance and UV-B damage in marine microphytobenthic communities. *Aquat. Microb. Ecol.* 52, 223–232. <https://doi.org/10.3354/ame01218>
- Mus, F., Toussaint, J.P., Cooksey, K.E., Fields, M.W., Gerlach, R., Peyton, B.M., Carlson, R.P., 2013. Physiological and molecular analysis of carbon source supplementation and pH stress-induced lipid accumulation in the marine diatom *Phaeodactylum tricorutum*. *Appl. Microbiol. Biotechnol.* 97, 3625–3642. <https://doi.org/10.1007/s00253-013-4747-7>
- Nassiry, M., Aubert, C., Mouzdahir, A., Rontani, J.F., 2009. Generation of isoprenoid compounds, notably prist-1-ene, via photo- and autoxidative degradation of vitamin E. *Org. Geochem.* 40, 38–50. <https://doi.org/10.1016/J.ORGGEOCHEM.2008.09.009>
- Niklas, K.J., Cobb, E.D., Matas, A.J., 2017. The evolution of hydrophobic cell wall biopolymers: from algae to angiosperms. *J. Exp. Bot.* 68, 5261–5269. <https://doi.org/10.1093/JXB/ERX215>

- Ntougias, Spyridon, Russell, N.J., Ntougias, S, Russell, · N J, 2000. *Bacillus* sp. WW3-SN6, a novel facultatively alkaliphilic bacterium isolated from the washwaters of edible olives. *Extrem.* 2000 44 4, 201–208. <https://doi.org/10.1007/PL00010712>
- Nyssen, F., Brey, T., Dauby, P., Graeve, M., 2005. Trophic position of Antarctic amphipods - Enhanced analysis by a 2- dimensional biomarker assay. *Mar. Ecol. Prog. Ser.* 300, 135–145. <https://doi.org/10.3354/meps300135>
- Patel, A., Arora, N., Sartaj, K., Pruthi, V., Pruthi, P.A., 2016. Sustainable biodiesel production from oleaginous yeasts utilizing hydrolysates of various non-edible lignocellulosic biomasses. *Renew. Sustain. Energy Rev.* 62, 836–855. <https://doi.org/10.1016/j.rser.2016.05.014>
- Perkins, R.G., Lavaud, J., Serôdio, J., Mouget, J.L., Cartaxana, P., Rosa, P., Barille, L., Brotas, V., Jesus, B.M., 2010. Vertical cell movement is a primary response of intertidal benthic biofilms to increasing light dose. *Mar. Ecol. Prog. Ser.* 416, 93–103. <https://doi.org/10.3354/meps08787>
- Piepho, M., Arts, M.T., Wacker, A., 2012. Species-specific variation in fatty acid concentrations of four phytoplankton species: Does phosphorus supply influence the effect of light intensity or temperature? *J. Phycol.* 48, 64–73. <https://doi.org/10.1111/j.1529-8817.2011.01103.x>
- Pohl, C.H., Kock, J.L.F., 2014. Oxidized fatty acids as inter-kingdom signaling molecules. *Mol.* 2014, Vol. 19, Pages 1273-1285 19, 1273–1285. <https://doi.org/10.3390/MOLECULES19011273>
- Prasannabalaji, N., Ramya, V.P., Muralitharan, G., 2017. In vitro assessment of *Lyngbya* sp. and *Phormidium* sp. extracts for antibacterial and antioxidant properties 8, 16–29.
- Prelle, L.R., Karsten, U., 2022. Photosynthesis, respiration, and growth of five benthic diatom strains as a function of intermixing processes of coastal peatlands with the baltic sea. *Microorganisms* 10, 749. <https://doi.org/10.3390/microorganisms10040749>
- Prins, A., Deleris, P., Hubas, C., Jesus, B., 2020. Effect of light intensity and light quality on diatom behavioral and physiological photoprotection. *Front. Mar. Sci.* 7, 1–17. <https://doi.org/10.3389/fmars.2020.00203>
- Radwan, S.S., Sorkhoh, N.A., 1993. Lipids of n-alkane-utilizing microorganisms and their application potential. *Adv. Appl. Microbiol.* 39, 29–90. [https://doi.org/10.1016/S0065-2164\(08\)70593-8](https://doi.org/10.1016/S0065-2164(08)70593-8)
- Ramachandra, T. V., Mahapatra, D.M., Karthick, B., Gordon, R., 2009. Milking diatoms for sustainable energy: Biochemical engineering versus gasoline-secreting diatom solar panels. *Ind. Eng. Chem. Res.* 48, 8769–8788. <https://doi.org/10.1021/ie900044j>
- Ray, A.J., Seaborn, G., Leffler, J.W., Wilde, S.B., Lawson, A., Browdy, C.L., 2010. Characterization of microbial communities in minimal-exchange, intensive aquaculture systems and the effects of suspended solids management. *Aquaculture* 310, 130–138. <https://doi.org/10.1016/j.aquaculture.2010.10.019>
- Renaud, S.M., Thinh, L. Van, Parry, D.L., 1999. The gross chemical composition and fatty acid composition of 18 species of tropical Australian microalgae for possible use in mariculture. *Aquaculture* 170, 147–159. [https://doi.org/10.1016/S0044-8486\(98\)00399-8](https://doi.org/10.1016/S0044-8486(98)00399-8)
- Robinson, N., Eglinton, G., 1990. Lipid chemistry of Icelandic hot spring microbial mats. *Org. Geochem.* 15, 291–298. [https://doi.org/10.1016/0146-6380\(90\)90007-M](https://doi.org/10.1016/0146-6380(90)90007-M)

- Rontani, J.F., Nassiry, M., Michotey, V., Guasco, S., Bonin, P., 2010. Formation of pristane from α -tocopherol under simulated anoxic sedimentary conditions: A combination of biotic and abiotic degradative processes. *Geochim. Cosmochim. Acta* 74, 252–263. <https://doi.org/10.1016/J.GCA.2009.09.028>
- Rontani, J.F., Volkman, J.K., 2003. Phytol degradation products as biogeochemical tracers in aquatic environments. *Org. Geochem.* 34, 1–35. [https://doi.org/10.1016/S0146-6380\(02\)00185-7](https://doi.org/10.1016/S0146-6380(02)00185-7)
- Roper, M.M., 2004. The isolation and characterisation of bacteria with the potential to degrade waxes that cause water repellency in sandy soils. *Soil Res.* 42, 427–434. <https://doi.org/10.1071/SR03153>
- Saburova, M.A., Polikarpov, I.G., 2003. Diatom activity within soft sediments: Behavioural and physiological processes. *Mar. Ecol. Prog. Ser.* 251, 115–126. <https://doi.org/10.3354/meps251115>
- Safavi, M., Jafari Olia, M.S., Abolhasani, M.H., Amini, M., Kianirad, M., 2021. Optimization of the culture medium and characterization of antioxidant compounds of a marine isolated microalga as a promising source in aquaculture feed. *Biocatal. Agric. Biotechnol.* 35, 102098. <https://doi.org/10.1016/J.BCAB.2021.102098>
- Schäfer, H., Abbas, B., Witte, H., Muyzer, G., 2002. Genetic diversity of “satellite” bacteria present in cultures of marine diatoms. *FEMS Microbiol. Ecol.* 42, 25–35. <https://doi.org/10.1111/J.1574-6941.2002.TB00992.X>
- Schirmer, A., Rude, M.A., Li, X., Popova, E., Del Cardayre, S.B., 2010. Microbial biosynthesis of alkanes. *Science* (80-.). 329, 559–562. <https://doi.org/10.1126/science.1187936>
- Schnurr, P.J., Drever, M.C., Kling, H.J., Elnor, R.W., Arts, M.T., 2019. Seasonal changes in fatty acid composition of estuarine intertidal biofilm: Implications for western sandpiper migration. *Estuar. Coast. Shelf Sci.* 224, 94–107. <https://doi.org/10.1016/j.ecss.2019.04.047>
- Schnurr, P.J., Espie, G.S., Allen, D.G., 2013. Algae biofilm growth and the potential to stimulate lipid accumulation through nutrient starvation. *Bioresour. Technol.* 136, 337–344. <https://doi.org/10.1016/j.biortech.2013.03.036>
- Serôdio, J., Coelho, H., Vieira, S., Cruz, S., 2006. Microphytobenthos vertical migratory photoresponse as characterised by light-response curves of surface biomass. *Estuar. Coast. Shelf Sci.* 68, 547–556. <https://doi.org/10.1016/j.ecss.2006.03.005>
- Serôdio, J., Ezequiel, J., Barnett, A., Mouget, J.L., Meléder, V., Laviale, M., Lavaud, J., 2012. Efficiency of photoprotection in microphytobenthos: role of vertical migration and the xanthophyll cycle against photoinhibition. *Aquat. Microb. Ecol.* 67, 161–175. <https://doi.org/10.3354/AME01591>
- Serôdio, J., Vieira, S., Cruz, S., 2008. Photosynthetic activity, photoprotection and photoinhibition in intertidal microphytobenthos as studied in situ using variable chlorophyll fluorescence. *Cont. Shelf Res.* 28, 1363–1375. <https://doi.org/10.1016/j.csr.2008.03.019>
- Shiea, J., Brassell, S.C., Ward, D.M., 1990. Mid-chain branched mono- and dimethyl alkanes in hot spring cyanobacterial mats: A direct biogenic source for branched alkanes in ancient sediments? *Org. Geochem.* 15, 223–231. [https://doi.org/10.1016/0146-6380\(90\)90001-G](https://doi.org/10.1016/0146-6380(90)90001-G)
- Silsbe, G.M., Kromkamp, J.C., 2012. Modeling the irradiance dependency of the quantum efficiency of photosynthesis. *Limnol. Oceanogr. Methods* 10, 645–652. <https://doi.org/10.4319/lom.2012.10.645>

- Singh, S.C., Sinha, R.P., Häder, D.-P., 2002. Role of lipids and fatty acids in stress tolerance in cyanobacteria. *Acta Protozool.* 41, 297–308.
- Sinninghe Damsté, J.S., Schouten, S., Rijpstra, W.I.C., Hopmans, E.C., Peletier, H., Gieskes, W.W.C., Geenevaesen, J.A.J., 2000. Novel polyunsaturated n-alkenes in the marine diatom *Rhizosolenia setigera*. *Eur. J. Biochem.* 267, 5727–5732. <https://doi.org/10.1046/J.1432-1327.2000.01636.X>
- Moulin, S.L.Y., Beyly-Adriano, A., Cuiné, S., Blangy, S., Légeret, B., Floriani, M., Burlacot, A., Sorigué, D., Samire, P.-P., Li-Beisson, Y., Peltier, G., Beisson, F., 2021. Fatty acid photodecarboxylase is an ancient photoenzyme that forms hydrocarbons in the thylakoids of algae. *Plant Physiol.* 186, 1455–1472. <https://doi.org/10.1093/plphys/kiab168>
- Soltani, M., Metzger, P., Largeau, C., 2004. Effects of hydrocarbon structure on fatty acid, fatty alcohol, and β -hydroxy acid composition in the hydrocarbon-degrading bacterium *Marinobacter hydrocarbonoclasticus*. *Lipids* 39, 491–505. <https://doi.org/10.1007/S11745-004-1256-9>
- Sorigué, D., Légeret, B., Cuiné, S., Blangy, S., Moulin, S., Billon, E., Richaud, P., Brugière, S., Couté, Y., Nurizzo, D., Müller, P., Brettel, K., Pignol, D., Arnoux, P., Li-Beisson, Y., Peltier, G., Beisson, F., 2017. An algal photoenzyme converts fatty acids to hydrocarbons. *Science* (80-). 357, 903–907.
- Sorigué, D., Légeret, B., Cuiné, S., Morales, P., Mirabella, B., Guédeney, G., Li-Beisson, Y., Jetter, R., Peltier, G., Beisson, F., 2016. Microalgae synthesize hydrocarbons from long-chain fatty acids via a light-dependent pathway. *Plant Physiol.* 171, 2393–2405. <https://doi.org/10.1104/PP.16.00462>
- Stodola, F.H., Deinema, M.H., Spencer, J.F., 1967. Extracellular lipids of yeasts. *Bacteriol. Rev.* 31, 194–213.
- Sutherland, I.W., 2017. EPS – a complex mixture, in: Flemming, H., Neu, T., Wingender, J. (Eds.), *The Perfect Slime: Microbial Extracellular Polymeric Substances (EPS)*. London: IWA Publishing, pp. 15–24.
- Underwood, G.J.C., Kromkamp, J., 1999. Primary production by phytoplankton and microphytobenthos in estuaries. *Adv. Ecol. Res.* 29, 93–153. [https://doi.org/10.1016/S0065-2504\(08\)60192-0](https://doi.org/10.1016/S0065-2504(08)60192-0)
- Van Beilen, J.B., Funhoff, E.G., 2007. Alkane hydroxylases involved in microbial alkane degradation. *Appl. Microbiol. Biotechnol.* 74, 13–21. <https://doi.org/10.1007/S00253-006-0748-0/FIGURES/3>
- Van Den Dool, H., Dec. Kratz, P., 1963. A generalization of the retention index system including linear temperature programmed gas—liquid partition chromatography. *J. Chromatogr. A* 11, 463–471. [https://doi.org/10.1016/S0021-9673\(01\)80947-X](https://doi.org/10.1016/S0021-9673(01)80947-X)
- Van Duyl, F.C., De Winder, B., Kop, A.J., Wollenzien, U., 1999. Tidal coupling between carbohydrate concentrations and bacterial activities in diatom-inhabited intertidal mudflats. *Mar. Ecol. Prog. Ser.* 191, 19–32. <https://doi.org/10.3354/meps191019>
- Véra, A., Desvillettes, C., Bec, A., Bourdier, G., 2001. Fatty acid composition of freshwater heterotrophic flagellates: An experimental study. *Aquat. Microb. Ecol.* 25, 271–279. <https://doi.org/10.3354/ame025271>
- Wainman, B.C., Smith, R.E.H., Rai, H., Furgal, J.A., 1999. Irradiance and lipid production in natural algal populations, in: Arts, M.T., Al., E. (Eds.), *Lipids in Freshwater Ecosystems*. pp. 45–70. https://doi.org/10.1007/978-1-4612-0547-0_4

- Wang, D., Zhou, S., Liu, L., Du, L., Wang, J., Huang, Z., Ma, L., Ding, S., Zhang, D., Wang, R., Jin, Y., Xia, C., 2015. The influence of different hydroponic conditions on thorium uptake by *Brassica juncea* var. *foliosa*. *Environ. Sci. Pollut. Res.* 22, 6941–6949. <https://doi.org/10.1007/s11356-014-3914-4>
- Waring, J., Baker, N.R., Underwood, G.J.C., 2007. Responses of estuarine intertidal microphytobenthic algal assemblages to enhanced ultraviolet B radiation. *Glob. Chang. Biol.* 13, 1398–1413. <https://doi.org/10.1111/j.1365-2486.2007.01378.x>
- Werner, U., Billerbeck, M., Polerecky, L., Franke, U., Huettel, M., Van Beusekom, J.E.E., De Beer, D., 2006. Spatial and temporal patterns of mineralization rates and oxygen distribution in a permeable intertidal sand flat (Sylt, Germany). *Limnol. Oceanogr.* 51, 2549–2563. <https://doi.org/10.4319/lo.2006.51.6.2549>
- Wiltshire, K.H., 2000. Algae and associated pigments of intertidal sediments, new observations and methods. *Limnologica* 30, 205–214. [https://doi.org/10.1016/S0075-9511\(00\)80017-1](https://doi.org/10.1016/S0075-9511(00)80017-1)
- Wotton, R.S., 2004. The ubiquity and many roles of exopolymers (EPS) in aquatic systems. *Sci. Mar.* 68, 13–21.
- Yamamori, T., Kageyama, H., Tanaka, Y., Takabe, T., 2018. Requirement of alkanes for salt tolerance of Cyanobacteria: characterization of alkane synthesis genes from salt-sensitive *Synechococcus elongatus* PCC7942 and salt-tolerant *Aphanothece halophytica*. *Lett. Appl. Microbiol.* 67, 299–305. <https://doi.org/10.1111/LAM.13038>
- Yeats, T.H., Rose, J.K.C., 2013. The formation and function of plant cuticles. *Plant Physiol.* 163, 5–20. <https://doi.org/10.1104/PP.113.222737>
- Zhukova, N. V., Kharlamenko, V.I., 1999. Sources of essential fatty acids in the marine microbial loop. *Aquat. Microb. Ecol.* 17, 153–157. <https://doi.org/10.3354/ame017153>

Statements and Declarations

Funding

This study was funded by the Regional Council of French Brittany, the General Council of Finistère.

Competing interests

The authors declare that they have no known competing financial interests or personal relationships that could have appeared to influence the work reported in this paper.

Author contributions

Caroline Doose is a postdoctoral researcher and lead author. She was in charge of conducting the experiments, interpreting data and writing of the first draft. Cédric Hubas is the supervisor and contributed to the experimental design, data interpretation and paper review.

Data availability statement

The data presented in this study and the R script use to analyze them are available on request from the corresponding author.

Figures

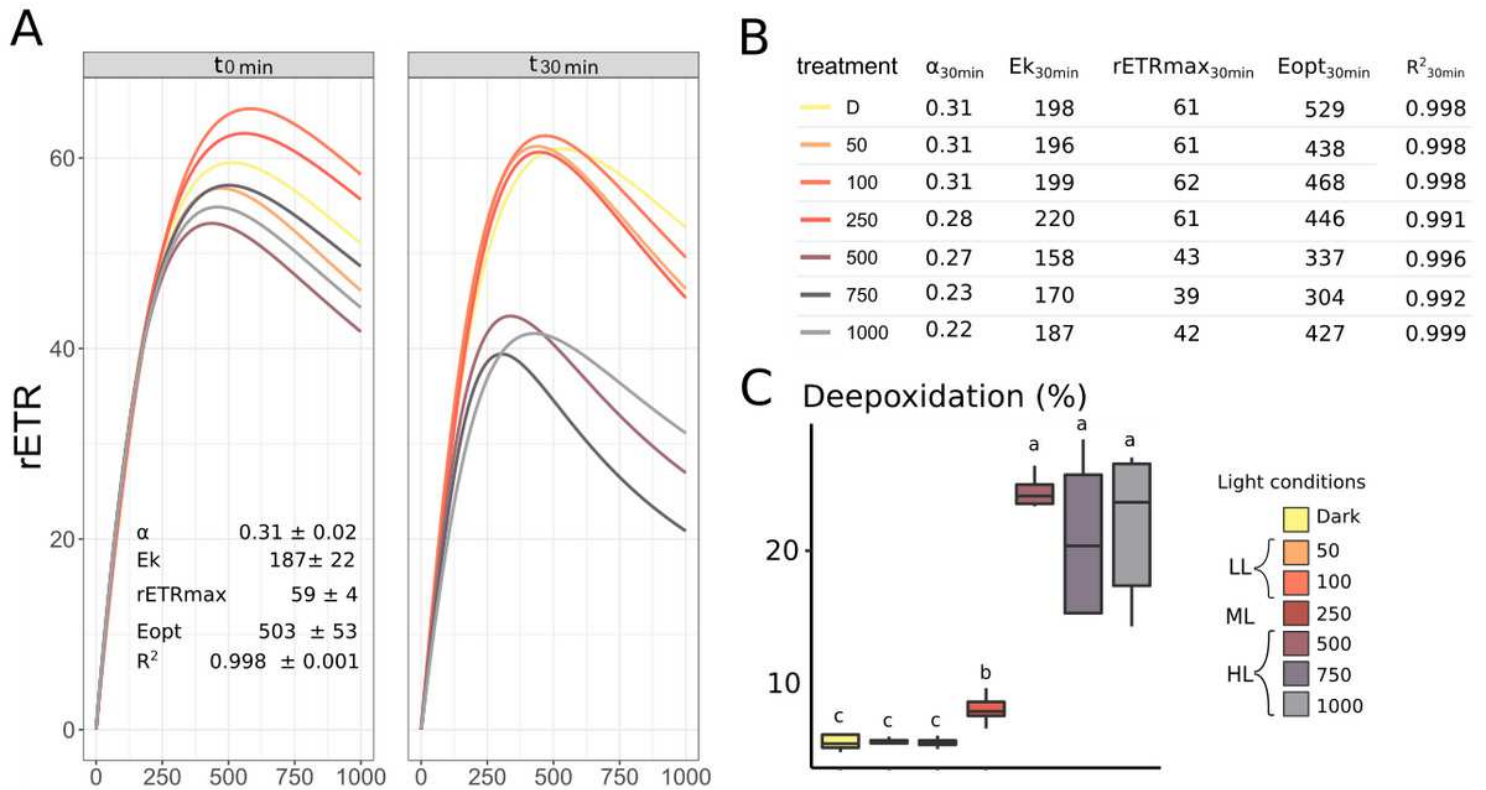


Figure 1

Fig 1 A. Light response curves (LCs) of the relative electron transport rate (rETR) of MPB biofilm at the experiment beginning t_0 and after 30 min (t_{30min}) ($n=1$) of dark (D) and of 50, 100, 250, 500, 750, 1000 $\mu\text{mol photons m}^{-2} \text{s}^{-1}$ PAR light exposure. Curves represent the model of Eilers and Peeters (1988) fitted to each data conditions and permitted to calculate the relative maximum electron transport rate ($rETR_{max}$), coefficient of light use efficiency (α), light saturation coefficient (E_k), optimal light parameter (E_{opt}) and the coefficient of determination (R^2). The t_0 LCs' parameters were statistically treated as replicates ($n=7$) **B.** LC parameters for the MPB biofilm at t_{30min} . **C.** De-oxidation state index ($DT/(DD+DT) \times 100$, mean \pm standard error) of biofilm exposed 30 min to dark (D) and to irradiances of 50, 100, 250, 500, 750, 1000 $\mu\text{mol photons m}^{-2} \text{s}^{-1}$ PAR. A Van der Waerden test was performed to detect significant differences between treatments, as indicated by letters ($p < 0.05$; $n = 5$). The letters correspond to treatment groups which were then used to distinguish light levels as follows: a = high light (HL), b = medium light (ML) and c = low light (LL)

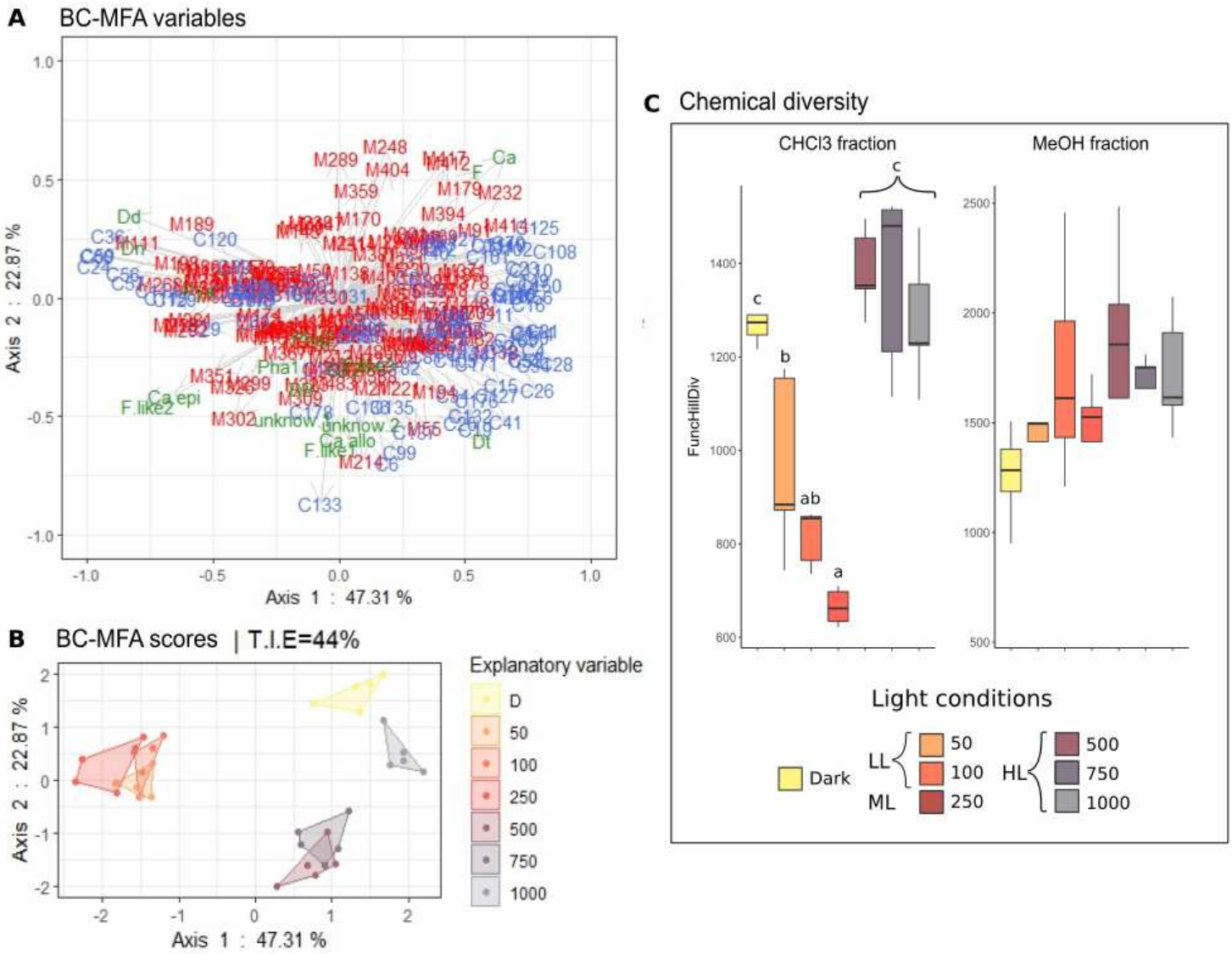


Figure 2

Fig. 2. A and B. Between Class (BC) analysis realized on a Multiple Factor Analysis (MFA) object (BC-MFA) on pigments, molecules obtained in the CHCl_3 (C) and MeOH (M), and **C.** chemical diversity in biofilm exposed to dark (D) and to irradiances of 50, 100, 250, 500, 750, 1000 $\mu\text{mol photons m}^{-2} \text{s}^{-1}$ PAR ($n=5$)

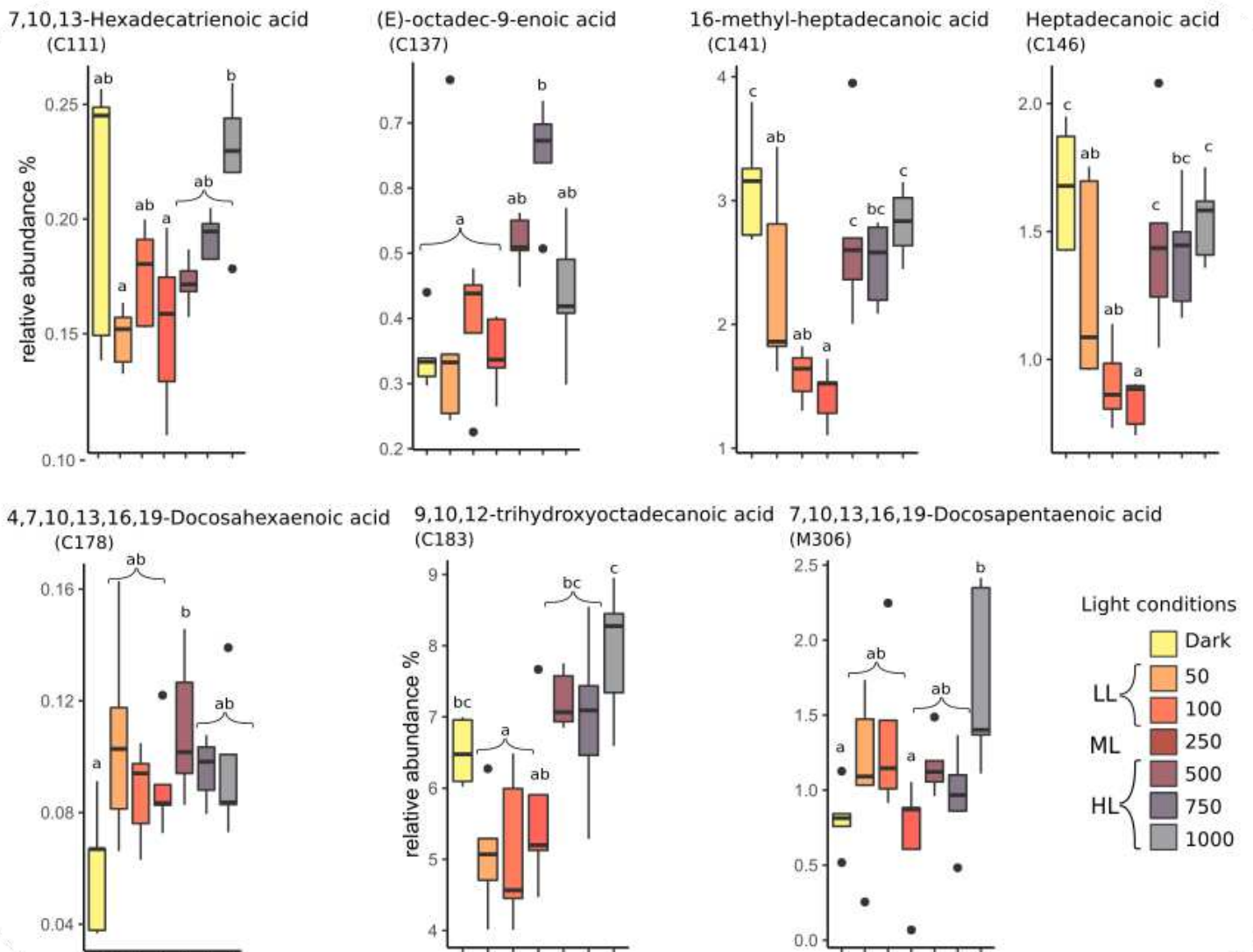


Figure 3

Fig.3 Fatty acids (FAs) measured in $CHCl_3$ (C) and MeOH (M) fractions in significantly higher values in biofilm exposed 30 min to LL (50 and 100 $\mu\text{mol photons m}^{-2} \text{s}^{-1}$ PAR) and ML (250 $\mu\text{mol photons m}^{-2} \text{s}^{-1}$ PAR) than in dark (D) and HL (500, 750, 1000 $\mu\text{mol photons m}^{-2} \text{s}^{-1}$ PAR). A one-way ANOVA was performed on the 7,10,13-Hexadecatrienoic acid (C16:3n-3; C111), The 16-methyl-heptadecanoic acid (iso-C18:0; C141), the heptadecanoic acid (C17:0; 146), the 4,7,10,13,16,19-Docosahexaenoic acid (C22:6n-3, DHA; C178), the 9,10,12-trihydroxyoctadecanoic acid (C183) and 7,10,13,16,19-Docosapentaenoic acid (22:5n-3, DPA; M306) data to detect significant differences between treatments, as indicated by letters ($p < 0.05$; $n = 5$)

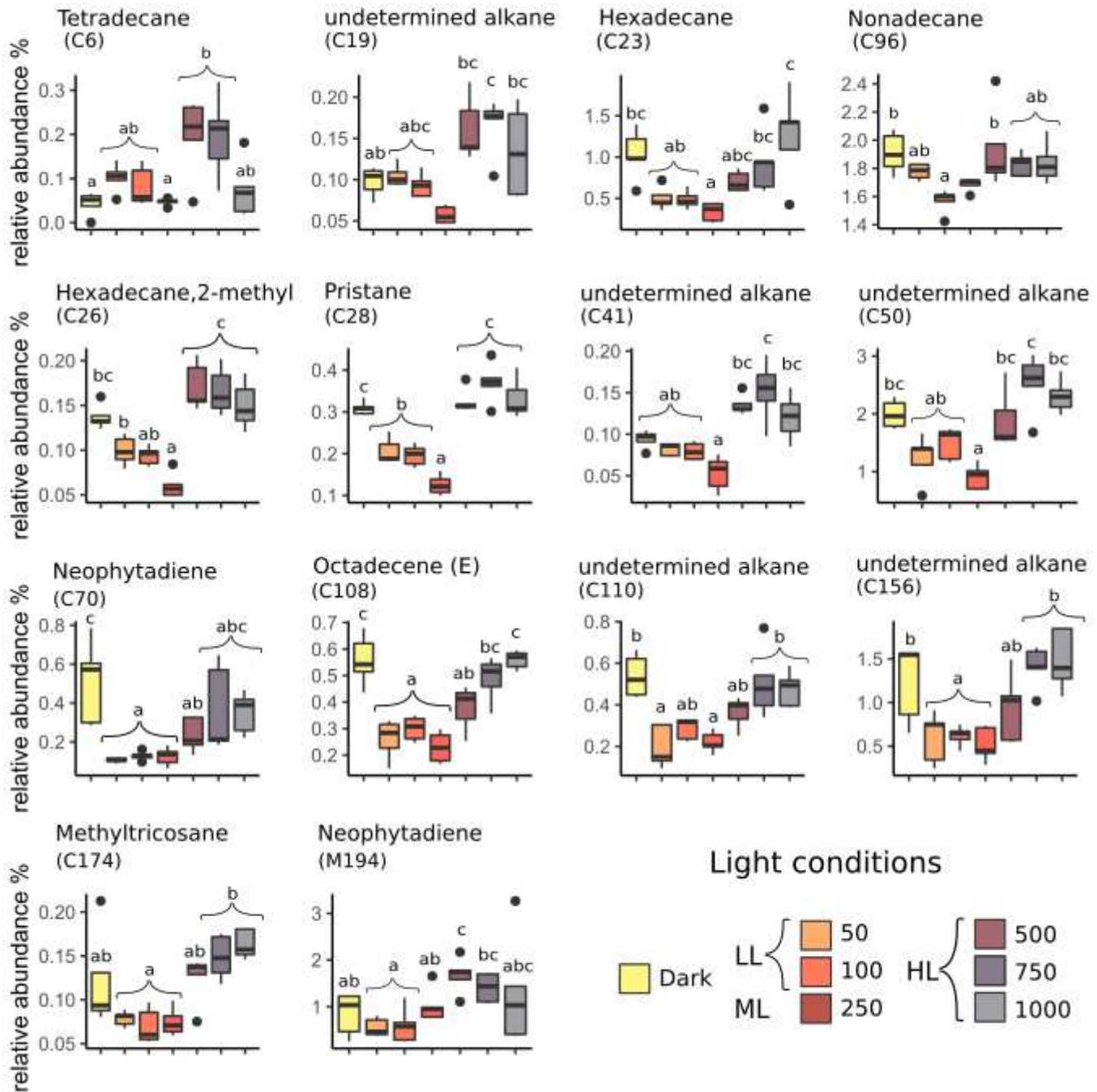


Figure 4

Fig. 4 Alka(e)nes measured in CHCl_3 fractions which significantly varied in biofilm exposed 30 min to dark (D) and to irradiances of 50, 100, 250, 500, 750, 1000 $\mu\text{mol photons m}^{-2} \text{s}^{-1}$ PAR. A one-way ANOVA was performed for Tetradecane (C6), Hexadecane (C23), Nonadecane (C96), Pristane (C28), Hexadecane,2-methyl (C26), Neophytadiene (C70 and M194), Octadecene (E) (C108) and the undetermined alkanes (C19, C41, C50, C110 and C156) data, and a Van der Waerden test was performed on 2-Methyltricosane (C174) data to detect significant differences between treatments, as indicated by letters ($p < 0.05$; $n = 5$)

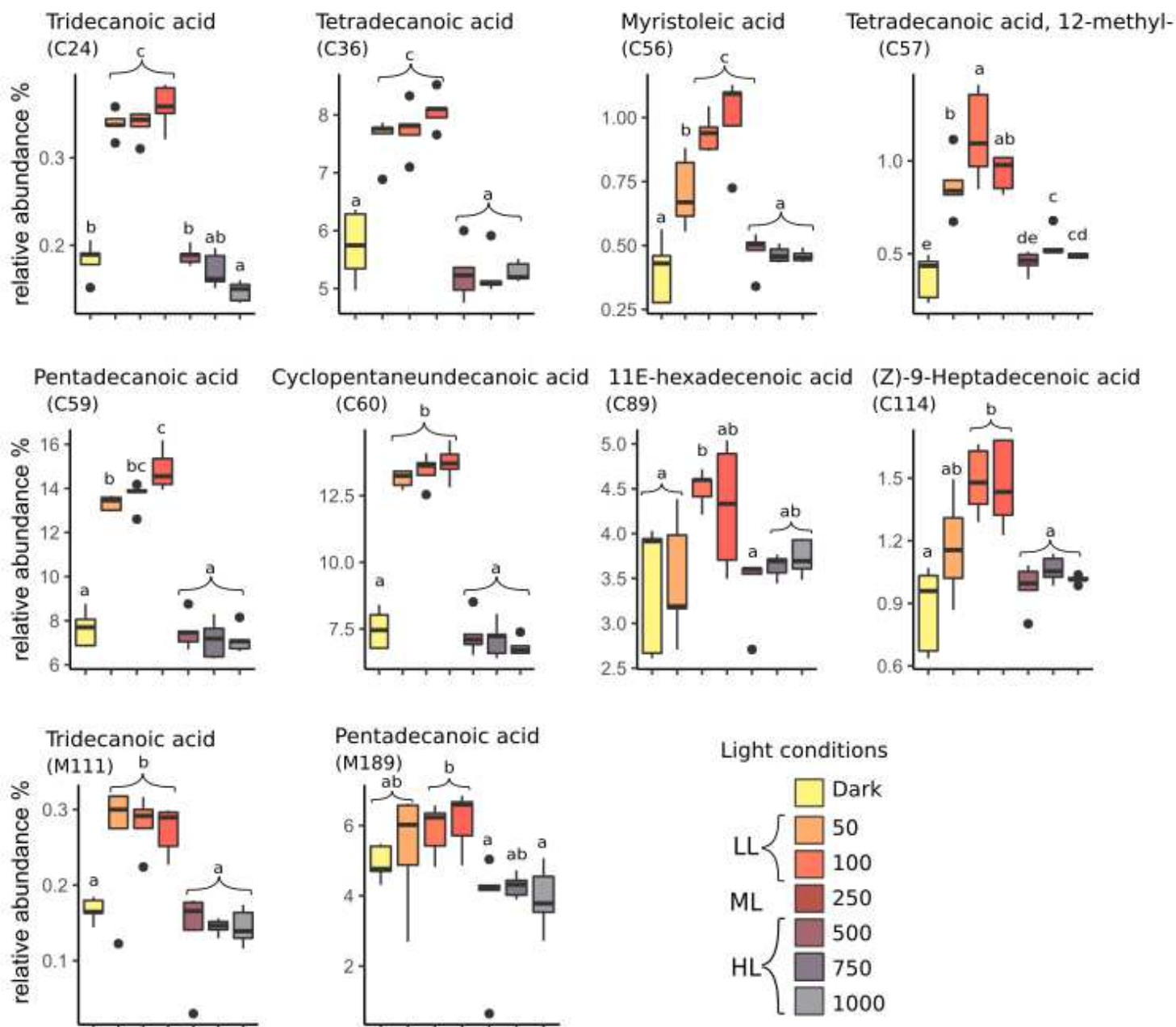


Figure 5

Fig.5 Fatty acids (FAs) measured in CHCl_3 (C) and MeOH (M) fractions in significantly higher values in biofilm exposed 30 min to LL (50 and 100 $\mu\text{mol photons m}^{-2} \text{s}^{-1}$ PAR) and ML (250 $\mu\text{mol photons m}^{-2} \text{s}^{-1}$ PAR) than in dark (D) and HL (500, 750, 1000 $\mu\text{mol photons m}^{-2} \text{s}^{-1}$ PAR). A one-way ANOVA was performed on the tridecanoic acid (C13:0; C24), the tetradecanoic acid (C14:0; C36), the myristoleic acid (C14:1-n5; C56), the pentadecanoic acid (C15:0; C59 and M189), the cyclopentaneundecanoic acid (C60), the 11E-hexadecenoic acid (C16:1-n5; C89), and the (Z)-9-Heptadecenoic acid (C17:1n-8; C114) data, and a Van der Waerden test was performed on the 12-methyltetradecanoic acid (C57; anteiso-C15:0) and the tridecanoic acid (C13:0; M111) to detect significant differences between treatments, as indicated by letters ($p < 0.05$; $n = 5$)

Supplementary Files

This is a list of supplementary files associated with this preprint. Click to download.

- [MigFe2021F02.png](#)
- [PigPercBiof.png](#)